LAPPEENRANTA-LAHTI UNIVERSITY OF TECHNOLOGY
School of Energy Systems
Energy Technology

Measurement system design for a two-stage dry screw air compressor and a pre-test uncertainty estimation for the measurement system

Supervisors: Prof. Teemu Turunen-Saaresti
D.Sc. (Tech.) Jonna Tiainen

Lappeenranta 07.09.2020

Abiola Oladejo

ABSTRACT

Lappeenranta-Lahti University of Technology
LUT School of Energy Systems
Energy Technology

Abiola Oladejo

Measurement system design for a two-stage dry screw air compressor and a pre-test uncertainty estimation for the measurement system

2020
Master's thesis
64 pages, 20 figures, 7 tables, and 1 appendix

Supervisors: Prof. Teemu Turunen-Saaresti
D.Sc. (Tech.) Jonna Tiainen

Keywords: dry screw compressor, efficiency, uncertainty, measurement, mass flow

About 10% of industrial electricity usage is attributed to compressed air systems. Dry screw compressors especially have a wide range of applications in many industries. However, many industries using dry screw compressors do not quantify the efficiency and performance of their screw compressors towards enabling energy savings. This thesis thus investigates alternative measurement setups that can be used for conducting a performance test for isentropic efficiency determination in a two-stage dry screw compressor with liquid cooling.

The findings of this thesis showed that isentropic efficiency of a compressor can be determined with and without internal compressor unit measurements. However, measurements inside a compressor unit are needed to properly estimate isentropic efficiency. When internal compressor unit measurements are not done, there are many unknowns and factors ignored; this may dispute the reliability of the efficiency result. Also, the use of flowmeters with long meter runs are not feasible to construct or mount in the industries due to space constraints. Therefore, a setup that uses a Coriolis meter with a suitable configuration was found to be an optimal design. An Excel calculation tool was made which calculated the isentropic efficiency and the uncertainties associated with making the measurements.

ACKNOWLEDGEMENTS

This thesis was carried out in the Laboratory of Fluid Dynamics in Lappeenranta-Lahti University of Technology as part of an independent research project.

My sincere gratitude goes to Professor Teemu Turunen-Saaresti for the opportunity to write this thesis and his supervision. His guidance and useful assessment all along helped to ensure that the aims of this thesis were met.

I would like to thank D.Sc. (Tech.) Jonna Tiainen for her valuable assistance and supervision during this thesis. She was always willing to give her time to help and give constructive recommendations during the thesis.

Finally, I would also like to thank my family for their moral support during the period of writing this thesis, especially in the final months.

TABLE OF CONTENT

ABSTRACT

ACKNOWLEDGEMENTS

TABLE OF CONTENT

SYMBOLS AND ABBREVIATIONS

SYMBOLS AND ABBREVIATIONS

Latin alphabet

D	pipe diameter	m
k	coverage factor	-
N	rotational speed	rpm
P	power	kW
p	pressure	bar, kPa, hPa
q_m	mass flow	kg/s
q_v	volume flow	m^3/s
R	gas constant	kJ/kgK
r	radius	mm
s	entropy	kJ/kgK
T	temperature	ºC, K
u	standard uncertainty	-
$u_{\bar{x}}$	uncertainty of the mean	-
U	expanded uncertainty	-
$\dot{W}$	input power	kW

Greek alphabet

β	beta	-
η	efficiency	%
κ	isentropic exponent	-
π	pressure ratio	-

Subscripts

1	inlet
2	outlet
act	actual
amb.	ambient conditions
da	dry air

dry	dry compressed air
first	first stage
is	isentropic
mA	milliamp
mix	mixture
motor	motor
ref	reference conditions
second	second stage
sv	saturated vapor
vp	vapor
wet	wet compressed air
95	95% confidence interval

Abbreviations

ASME	American Society of Mechanical Engineers
DP	Differential Pressure
EU	European Union
FS	Full Scale
min.	minimum
o.r	of reading
PTC	Performance Test Code
P&ID	Piping and instrumentation diagram
RH	Relative humidity
RTD	Resistance Temperature Detector
SDGs	Sustainable Development Goals
SRM	Svenska Rotor Maskiner AB
USM	Ultrasonic meter
VSD	Variable Speed Drive

1 INTRODUCTION

Energy efficiency improvements are important for sustainable development as highlighted in the “Affordable and Clean energy” goal among the 17 Sustainable Development Goals (SDGs) set for 2030 by the United Nations (UN General Assembly, 2015). Improvements of 20% in energy efficiency is also one of the three main targets set by the European Union for 2020. Those targets have been updated to achieve a minimum of 32.5% in energy savings by 2030 (Tsemekidi-Tzeiranaki et al., 2018). For Finland to meet these energy efficiency targets, national targets have been set to limit the final energy consumption to 290 TWh by 2030. Of the total energy consumed in Finland, industries consume about 50% when running at full capacity (Finnish Ministry of Economic Affairs and Employment, 2019). Thus, industries need to be more efficient in their processes in order to reduce electricity consumption and contribute towards the energy efficiency goals.

Many industries use air compressors in their manufacturing process and this is why about 10% of electricity consumption is attributed to compressed air systems (U.S. Department of Energy, 2014). This shows the importance of compressed air systems and thus, the need for determining the efficiency of air compressors. Air compressors are of different types; axial, centrifugal, reciprocating, and screw compressors. Screw compressors can be oil-free (dry) or oil-injected compressors. The dry screw compressors are the main focus of this thesis. Dry screw compressors are generally essential in industrial applications that require oil-free air to prevent contamination such as in food and beverage, automotive, pharmaceuticals, pulp and paper, cosmetics, textiles, and electronics industries. (Kovacevic et al, 2007.)

Dry screw compressors comprise of coated rotors in a compression chamber with air gaps between the rotors which sucks in air and compresses the air. Teflon (Polytetrafluoroethylene) is used as a coating material for the rotors because of its non-stick and non-reactive nature. Even though the rotors do not touch, the teflon wears over time as a result of the air compression process. In the compression system, there is an oil circuit for lubricating the gears that drive the rotors. Seals help to prevent air in the compression chamber from getting into the oil circuit. The seals also prevent oil from getting into the compression chamber in order for the compressed air to be used in various industrial applications that need an oil-free air. (Kovacevic et al, 2007.)

Dry screw compressor efficiency can be affected by various factors. The factors may include compressor age, the extent of operation hours, ambient conditions, how much the teflon wears, frequency of refurbishment, fixed speed or variable speed drive, start-stop use, etc. Therefore, conditions under which these compressors operate need to be known to estimate the efficiency of the dry screw compressor and to compare compressor units with each other. This thesis is thus the first step in determining the measurements needed for dry screw compressor efficiency calculations.

1.1 Objectives of the thesis

This thesis focuses on a two-stage dry screw compressor technology with liquid cooling. The objectives of this thesis are:

1. To understand the operation of two-stage dry screw compressors
2. To determine an optimal measurement system design for determining the efficiency of dry screw compressors
3. To determine and analyze the measurement system uncertainty

Dry screw compressors do not inject oil into the compression chamber, hence, why they are also known as oil-free screw compressors. To understand the concept of dry screw compressors, theoretical research was done on dry screw compressors with liquid cooling. Ambient conditions and the cooling of the compressed air affects the efficiency of the dry screw compressors, hence, certain parameters and quantities need to be measured. In order to determine an optimal measurement system design, four different piping configuration systems based on three flowmeter options were investigated. The piping configurations were compared based on compactness, accuracy, feasibility to mount in factories, amongst other considerations. In addition, three levels or scenarios of measurements were considered based on the complexity of measurements that can be carried out. An estimation of the measurement uncertainties was carried out for the three scenarios. The feasibility, advantages, and disadvantages of the piping configuration and measurement scenarios were analyzed in order to recommend a suitable measurement design for dry screw compressors.

1.2 Structure of the thesis

Chapter 1 of this thesis gives general knowledge on energy efficiency and the targets set at the national, EU, and global levels. General discussion on dry screw compressors and their

use in industrial processes is included. This chapter briefly discusses the need for estimating compressor efficiency. This chapter also outlines the objectives and structure of the thesis.

Chapter 2 of this thesis describes the development of dry screws, their applications, working principle, variable speed drives and fixed speed drives, leakages in the screw compressor chamber, and how the leakages affect efficiency. Two-stage compressors with cooling systems were also explained.

Chapter 3 of this thesis includes a review of the standards related to compressor performance test and the measurements necessary for efficiency analysis were discussed. The operating principle of selected flowmeters which can be used for flow measurement were also discussed. The inlet and different outlet measurement options possible based on the flowmeter options. For the compressor outlet measurements, three flowmeter technologies and how they affect the piping configuration design were considered. An initial comparison of the designs was also done.

Chapter 4 of this thesis includes the description of the typical dry screw compressor unit using an ideal P&ID. Three measurement scenarios were assessed based on the possible measurements inside the compressor unit. The steps followed in the calculation system for efficiency determination and calculations back to reference conditions were also included in the chapter.

Chapter 5 of this thesis includes some knowledge of uncertainty principles and uncertainty in measurement systems. The types of evaluation used in the measurement uncertainty estimation, the steps followed in determining the expanded uncertainty and the calculation process was also explained. The results of the uncertainty in the efficiency, mass flow rate, and pressure ratio were included. The uncertainty when the mass flow, rotational speed, and power were calculated back to reference conditions was also done. How a change in ambient temperature affects the measurement uncertainty is included in this chapter.

Chapter 6 of this thesis entails discussion and comparisons between the measurement system designs and measurement scenarios. Comparisons were done based on their advantages and weaknesses in order to make recommendations for the most suitable option. Some suggestions for further research in this topic area was briefly discussed.

2 DRY SCREW COMPRESSORS

Since dry screw compressors are the focus in this thesis, its principle of operation and literature review on this type of compressors are researched.

2.1 Brief historical development of dry screw compressors

Although the idea of screw compressors was first discovered in Germany in 1878, it was not until Alf Lysholm, a Chief Engineer at Svenska Rotor Maskiner AB (SRM) developed the concept of dry screw compressors in 1934 as part of the development of gas turbines. The first dry screw designs had asymmetric profiles, which led to over-compression as a result of trapped pockets. However, circular symmetric profiles were introduced by SRM as a development in the early 1950s to increase efficiency by eliminating the trapped pockets. Several configurations were tested but the standard symmetric profiles of four male and six female rotors (4+6 lobe combination) were proposed. The lobe combination was suitable for a wide range of compression ratio and tip speed. It also helped to reduce sealing edge damages that can be caused by thermal expansion or poor rotor timing. (Svenningson et al., 2010; Brown 2011.)

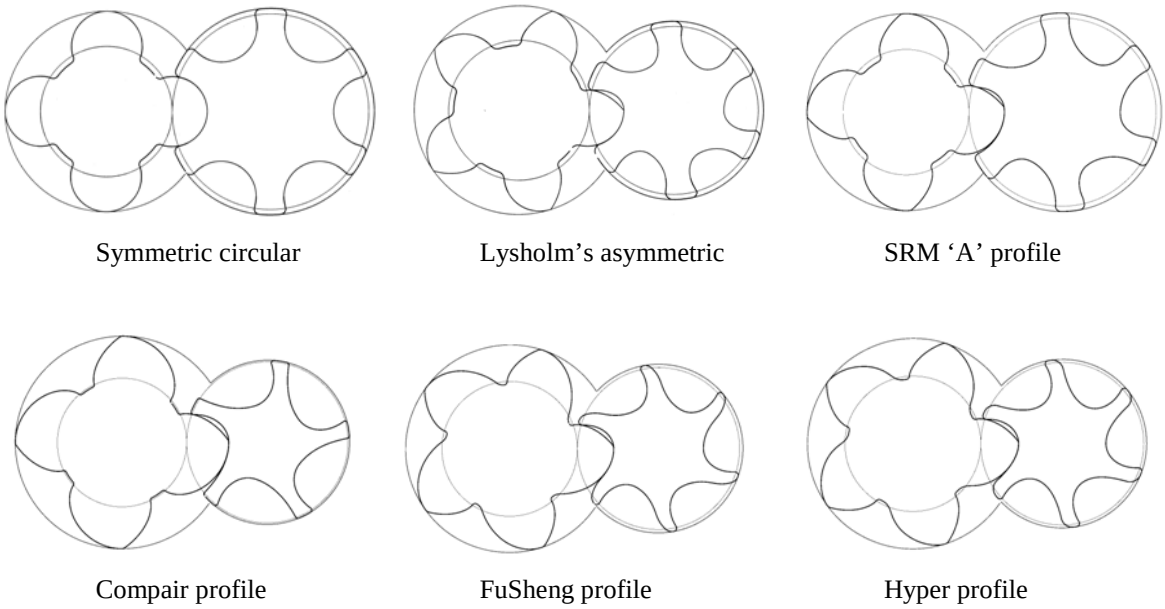

Figure 1. Some of the most popular screw compressor rotors (Stosic et al., 2011).

Developments and modifications have been made to the rotor profiles in modern screw compressors as shown in Figure 1 but the asymmetric 4+6 combination is the most commonly used in dry screw compressors. There are also 3+5 lobe combinations that are used in low-

pressure processes and applications (Wennemar, 2009). Dry screw compressors can come in a compressor unit, which consists of the package of the dry screw compressor elements, electric motor, automation components, oil circuit, filters, pumps, valves, controllers, cooling system and all necessary components needed to complete the unit.

2.2 Principle of operation

Dry screw compressor combines the principle of operation of a reciprocating compressor (positive displacement) and a centrifugal compressor (rotary motion). Air is sucked into the compressor that contains a male and a female rotor for compression as the air moves towards the discharge. The rotary motion ensures that air is being compressed as the temperature and pressure increase while the volume of the gas decreases. The rotors are driven by external timing gears, which helps to keep the male and female rotors from being in contact. There are bearings at the ends of the shaft, and shaft seals are used to prevent external oil (used for lubricating the bearing) from getting into the compression chamber. In dry screw compressors, there are tight clearances that are enough to prevent the rotors from touching each other or from touching the compressor casing when there is thermal expansion resulting from the compression process. (Brown, 2011; Kovacevic et al, 2007.)

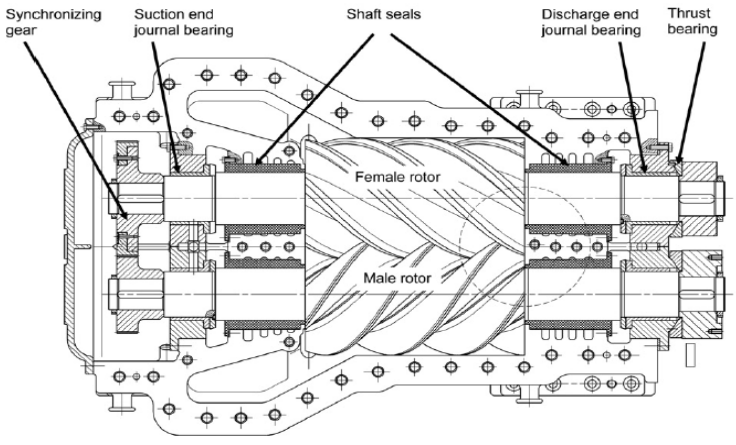

Figure 2. Dry screw compressor (Wennemar, 2009).

Figure 2 shows the horizontal section of a single-stage dry screw compressor and its main components. However, dry screw compressors can also be manufactured in multiple stages that have interstage. A two-stage compressor helps to reduce power consumption, reduce internal leakage losses, and prolong the lifetime of the bearings when running at full load.

The two-stage compressor is the most common multiple-stage design for dry screw compressors as shown in Figure 3 where a common drive is used for multiple pinions. (Wennemar, 2009; Sullair, 2012.)

A common driver can drive multiple-stage compressor sets. The driver can be either a fixed speed drive or a variable speed drive. The fixed speed drive (also called an idling compressor) can either operate at full load (when turned on) or no load at all (where it is turned off). A Variable Speed Drive (VSD) is an electric motor which allows control and variation of the rotational speed. VSDs help to drive the motor at a suitable speed for performance optimization based on the load. This thus helps to increase efficiency and reduce mechanical losses. In air compression systems, this capacity variation based on air demand helps in energy savings. (Saidur et al., 2012.)

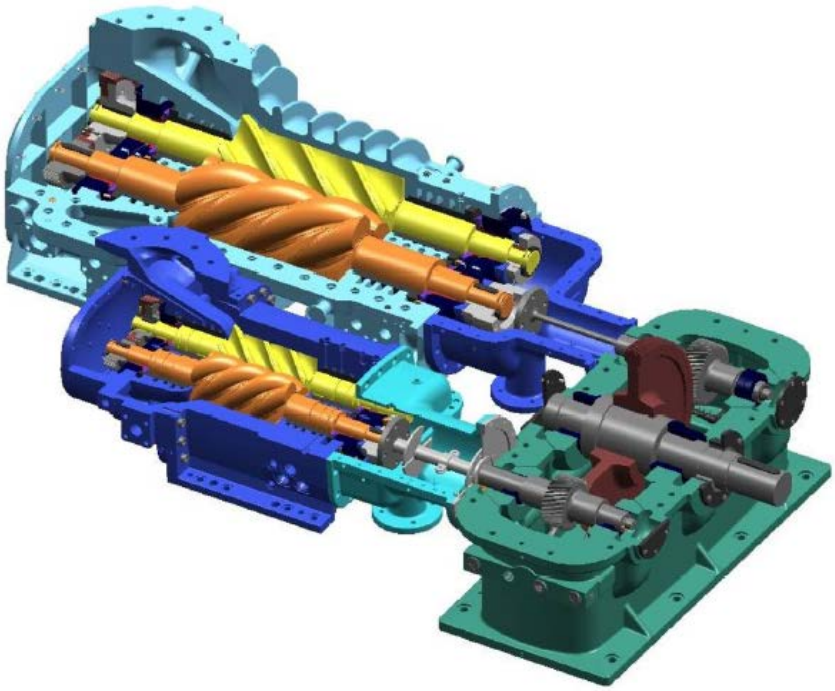

Figure 3. A typical two-stage compressor arrangement with individual pinions (Wennemar, 2009).

To ensure more energy savings and minimize the relative effect of leakage, there should be an increase in the capacity of the compressor flow that results from increasing the flow area between the lobes. Nowadays, during the design of dry screw compressors, the rotor profile can be optimized by making the male lobes larger and the female lobes thinner (this strengthens the female lobe). This essentially implies that the male and female interlobes should not be made too thick and too thin respectively. When this happens, it leads to a shorter sealing

line, less torque on the female rotor, better flow area, and reduced deformation of the female rotor from pressure. (Kovacevic et al, 2007.)

More spacing between the rotors and the presence of gears that drives the rotors outside the compression chamber leads to the oil-free compressors requiring larger casing than oil-injected compressors. If there are no optimal spacing in the screw compressors, then losses may occur. Losses in screw compressors can also occur by other means. Losses due to gas leakage may reduce the mass flow if there are large tip clearances. This subsequently affects the mass flow of gas from the suction chamber and the efficiency. There could also be losses from the compression chamber through the shaft seals (if seals are not fitted well for tightness). Also, there may be a reduction in compressor efficiency through discharge port losses if the discharge port location is too near or too far. If the discharge port is too near, it will lead to a decrease in the volumetric efficiency, whereas, if it is too far, it will lead to over-compression and thus power losses. (Kovacevic et al, 2007; Fofanov, 2015.)

There are states where under-compression and over-compression can occur. These two states can lead to efficiency loss and pulsation of gas at the discharge line. Under-compression occurs when the pressure in the compression chamber is less than the discharge pressure and it causes a backflow from the discharge. Whereas, over-compression results from higher compression pressure than discharge pressure which can subsequently lead to gas overheating in the compression chamber. (Wennemar, 2009.)

2.3 Two-stage compressor with water cooling system

Dry screw compressors are usually designed with two or three stages (mostly two stages in modern screw compressors). As the temperature and pressure of the gas increases due to compression, intercooling is needed between the stages in order to reduce the temperature at the second stage inlet. Intercooling between the first stage and second stage improves the efficiency of the compression process by increasing the density at the inlet of the second stage. Condensation thus results from the cooling of the compressed air. There are different types of cooling systems which are; open cooling system without circulating water, open cooling system with circulating water, and closed system. Open systems of cooling usually have lower initial costs but the running costs are high. (Atlas Copco, 2019.)

As air comes in through the compressor inlet, compression takes place in the first stage of the screw compressor. Liquid is then used to cool the air at intermediate pressure and to cool the oil used for lubricating the gears and bearings. The air exiting the first stage compressor undergoes intercooling, and condensation occurs. The condensate is then discharged through a valve at the condensate water separation. The second stage compression increases the air to its final pressure before it is cooled by the liquid in the aftercooler as shown in Figure 4. Moisture from the air is again collected as condensate water before the compressed air exits to the distribution lines. (Lazzarin et al., 2016.)

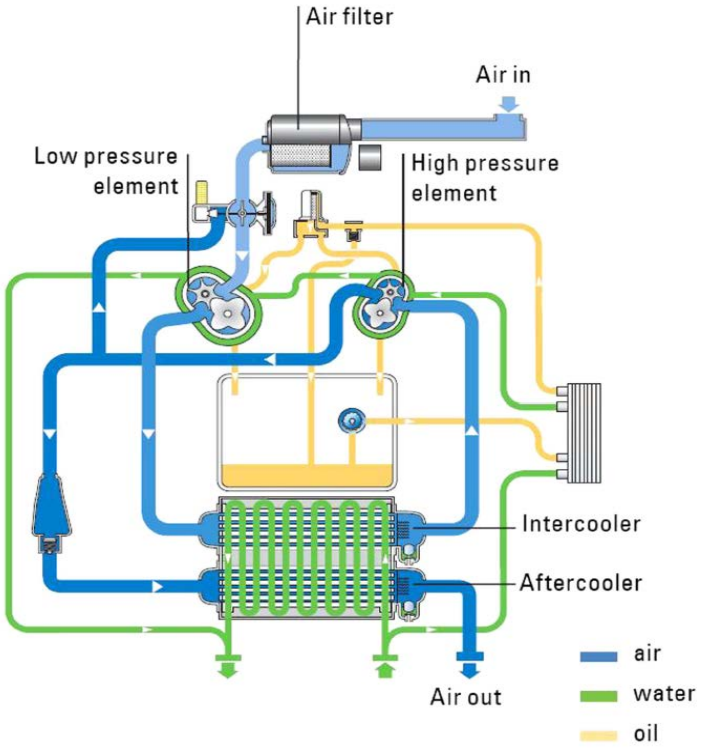

Figure 4. A two-stage screw compressor unit with water cooling (Lazzarin et al., 2016).

The aftercooler in Figure 4 helps to reduce the compressed air temperature, and water that would have otherwise ended up in the piping system can be removed. About 80-90% of condensate water can be collected in the separator at this stage. The temperature of compressed air exiting from the aftercooler is usually about 10 °C above the temperature of the coolant. (Atlas Copco, 2019.)

When dry air is needed, a dryer usually in the form of a refrigerant dryer or adsorption dryer condenses and removes water from the wet compressed air. The dryer removes moisture

from cold and hot air respectively from systems with and without an aftercooler. Dew point in adsorption dryers can usually be reached at -40 °C, which indicates that very dry air can be achieved. Overall, cooling of the compressed air helps to improve compressor efficiency. (Atlas Copco, 2019.)

In a compression stage, the mass flow rate remains constant (the mass flow rate at the inlet of the screw compressor stage is equal to the mass flow rate at the outlet of the stage). Otherwise, there are leakages in the compressor. Pressure and density will increase as compression increases. However, in a multistage compression, the mass flow into the first compressor is different from the mass flow into the second compressor because of cooling which results in the removal of condensation water.

3 MEASUREMENT SYSTEM DESIGN AND PIPING SETUP

3.1 Review of standards for measurements needed for compressor performance test

When conducting performance tests and analysis for compressors, various measurements need to be done. The properties of air at the compressor inlet and outlet, power to the compressor, and information on the cooling are needed to determine compressor efficiency. The details and information needed for the performance tests in this thesis are done according to two standards. The standards are ASME PTC 13-2018 (2019) (Wire-to-Air Performance Test Code for Blower Systems) and ASME PTC 10-1997 (1998) (Performance Test Code on Compressors and Exhausters).

When making measurements, ASME PTC 13-2018 (2019) indicates that data should be collected for each test point. A test point is the averaging of at least three readings after discarding any reading that falls outside the permissible fluctuation. This means that the average reading serves as a test point data. The duration for taking a test point data after stabilization should be at least 15 minutes from the start of the first reading set to the end of the third reading set of all instruments.

When multiple independent instruments are used for measuring pressure or temperature, any reading that is inconsistent with the permissible fluctuation should be eliminated before finding the average of a minimum of three readings. This average is then used as the measurement value of the temperature or pressure. Pressure can be measured by using instruments indicated in ASME PTC 19.2 (Pressure measurement). When measuring ambient pressure, measurement should be done at the inlet region without interference from weather or direct sunlight.

ASME PTC 13-2018 (2019) standard also indicates that temperature can be measured by using instruments indicated in ASME PTC 19.3 (Temperature measurement). It is important to insulate the pipe region from the outlet of the compressor to the temperature measurement and flow measurement locations. This is essential to reduce the thermal gradient in the airflow. When several measuring instruments are used, an average of the readings should be done.

In accordance with ASME PTC 13-2018 (2019), relative humidity should be measured at the inlet region where the inlet temperature was measured. This is to ensure that relative humidity (RH) is measured under the same conditions that are free from direct sunlight and fluctuations in temperature change. Rotational speed measurements should be done with instruments having an accuracy of at least 0.15% according to ASME PTC 13-2018 (2019). Shaft power can be measured in five different ways according to ASME PTC 10-1997 (1998). Shaft power can be measured directly using torque meters or reaction mounted drivers. Shaft power can also be computed by electrical input measurement to the driver motor, by heat balance measurements or evaluated by heat exchanger methods.

According to ASME PTC 13-2018 (2019), measurement of volumetric flow at the outlet of the compressor unit is recommended. This is to ensure the net delivered flow measured at the outlet can be converted into the inlet conditions that excludes the losses in the compression system. Losses in the compressor may be as a result of leakages, condensation, and other forms of leakages. Flow measurement should be done using differential pressure meters indicated in ASME PTC 13-2018 (2019), or using instruments that are in accordance with ASME PTC 19.5-2004 (Flow measurement) standard.

3.2 Flow measurement

When conducting performance tests for compressors, flow measurement is essential and the instrument used for measurement need to be chosen carefully. A selection of various flow measurement technologies was studied to understand their principle of operation, and for assessment of their usability and practicability to air compressor technology. When choosing a flowmeter, various factors need to be considered at different steps of the selection process. First, a list of available flowmeters for the application needs to be identified. Secondly, factors such as sizing, rangeability, cost, accuracy, operation and performance conditions help to narrow down the options to make the best available and suitable selection. (Lipták and Lomas, 2003.)

Research was done on flow measurement using differential pressure (DP) technology such as orifice plates, nozzles and Venturi nozzles, Venturi tubes, and cone meter. Research was also done on thermal flowmeters, Coriolis meters, and ultrasonic meters. However, based on meter accuracy, flow range, upstream meter run, applicability, constraints of mounting the flowmeter in the industry, feasibility, amongst other considerations, the following three flowmeters were chosen as alternatives that can be used. They are differential pressure cone meter, ultrasonic meter, and Coriolis meter. The principle of operation of the three flow measurement technologies is discussed.

3.2.1 Cone meter

Cone meter uses differential pressure (DP) technology for flow measurement. DP transducers are used for measuring reference pressure and measured pressure. From Figure 5, P1’ is the reference pressure that is measured on the upstream side of the cone. P2’ is measured via the cone in the throttling set inside the pipe. As air flows in the direction of the cone, the flow area reduces which thus increases the fluid velocity. This leads to an area of low pressure after the cone on the downstream. The pressure differential between the upstream and the downstream is then used to determine the flow rate of the fluid using Bernoulli’s equation which states that the pressure of a fluid is inversely proportional to the square root of the velocity in a closed pipe. This simply means that P1’ is the pressure of the fluid as it approaches or moves near the cone before the pressure drops to P2’ after the cone. Flow measurement with cone meter helps to remove result uncertainty brought about by swirl, less

noise signals, low pressure loss. Cone meters do not require a lot of straight pipe length to measure the flow. (McAllister, 2014; Dong et al., 2009.)

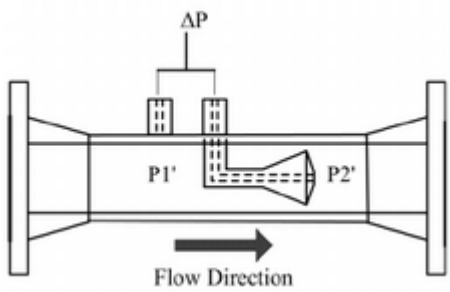

Figure 5. The structure of a cone meter (Dong et al., 2009).

In DP technologies, Beta-ratio (β-ratio) should be considered when choosing the cone meter. β-ratio is the ratio of the diameter of the flow restriction to the diameter of the pipe. Therefore, it is the ratio of the diameter or throat of the flow device to the inner diameter of the pipe. It can also be called the diameter ratio. (Lipták and Lomas, 2003; ISO 5167-1, 2003.) When using a cone meter as an option for flow measurement in compressed air systems, the β-ratio should be chosen such that the gas expansion factor generated is at least 0.84 (McCrometer, 2008). The β-ratio is related to the pressure drop in that the more the flow is restricted, the higher the pressure drop and vice versa. Therefore, low β-ratio leads to high pressure drop. (McCrometer, 2008.)

3.2.2 Ultrasonic Meter

The transit time ultrasonic meter is the type of flowmeter suitable for flow measurement in gas applications. Ultrasonic signals are transferred through the pipe wall from one transducer to the other through the path C in Figure 6. When flow is present in the medium, the signals in the direction of the flow are faster while the signals are slower when moving against the flow direction. The difference between the upstream and downstream velocities is used to determine the flow velocity. Therefore, the difference in transit time is directly proportional to the flow velocity. The volumetric flow of the fluid is then the product of the average velocity and the cross-sectional area. (Scelzo et al., 2005; Siev et al., 2003.)

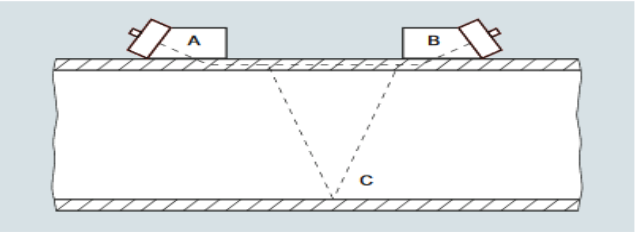

Figure 6. A multipath flow ultrasonic meter (Siemens, 2020).

The advantages of these ultrasonic flowmeters are that they cause little or no pressure drops and they have high accuracy. They may be expensive but they are able to operate over a wide range of pipe diameter.

3.2.3 Coriolis Meter

In a Coriolis flowmeter, there are usually two oscillating/vibrating tubes. When there is no mass flow, the two tubes are in phase or it could be said that they oscillate symmetrically. When there is mass flow, the two tubes oscillate asymmetrically. An electromagnetic driver between the two tubes in Figure 7 causes oscillation. Two motion sensors (one at the inlet side and the other at the outlet side of the tube) records the deformation and there is a phase shift or time delay between the first and the second sensor. The phase shift or time delay is directly proportional to the mass flow rate. In previous technologies, there have been issues related to flow measurement accuracy because of small Coriolis force as the phase shift depends on the driving frequency. Unlike phase shift, time delay does not depend on the driving frequency and this has helped to overcome the accuracy problems of phase shift. This development has provided a good basis for future development of Coriolis flowmeters. (Apple et al., 2003; Wang and Baker, 2014.)

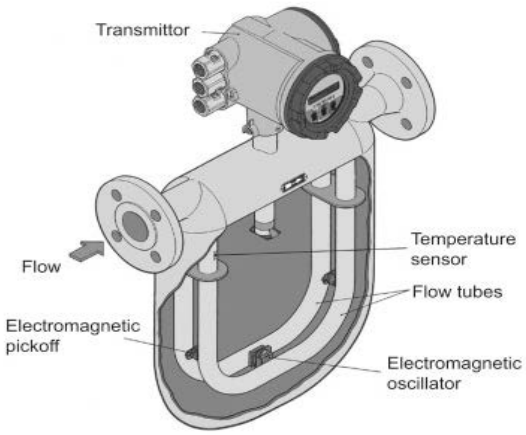

Figure 7. A Coriolis meter (Nakayama, 2018).

The temperature sensor in Figure 7 determines and measures the temperature of the flowing fluid. The temperature sensor is usually a resistance temperature detector (RTD) and it is an essential part of Coriolis meter designs (Wang and Baker, 2014). Overall, this technology has the advantage that temperature, density and mass flow (measured directly) can all be measured simultaneously. Also, Coriolis meters do not need inlet and outlet sections but may be sensitive to vibration if they are not installed properly. Coriolis flowmeters also require reduced maintenance and they have high accuracy. (ABB Automation Products GmbH, 2011.)

3.3 Measurement setup and piping configuration

According to ASME PTC 13-2018 (2019) and ISO 1217 (2009), several measurements as shown in Table 1 are needed when designing a measurement setup for dry screw compressors. The instruments chosen to measure these quantities are also shown in Table 1. ASME PTC 10-1997 (1998) indicates that measurement of the cooler inlet temperature, cooler outlet temperature, cooling fluid flow rate, and lubricant flows should be taken when applicable during the test.

Table 1. Measurements needed and the instruments chosen for making the measurements (ASME PTC 13-2018, ISO 1217)

Measurements	**Instruments chosen [Manufacturer, model]**
Ambient pressure	Barometer [Vaisala, BAROCAP digital barometer PTB330]
Inlet pressure and Outlet pressure	Pressure transmitter [GEFRAN, NaK filled melt pressure transmitters 4…20mA output]
Ambient temperature	Thermometer [WIKA, Hand-held thermometer CTH6300]
Inlet temperature and outlet temperature	Resistance temperature detectors [Texas Instruments, Pt 100 2- 3- 4- wire RTD]
Relative humidity	Hygrometer [PCE Instruments, Thermohygrometer PCE-555]
Power and rotational speed	Power analyzer
Flow rate	Cone meter [McCrometer, ExactSteam V-Cone flow meter] Ultrasonic meter [Transus Instruments, UIM4F] Coriolis meter [Tricor, TCM 028K]

According to ASME PTC 13-2018 (2019), pressure transmitters chosen should be according to the operating range of the compressor system. All instruments chosen should be calibrated according to the manufacturer's procedure and the standard instruments used for calibration should be approved by a national or international standard.

3.3.1 Inlet Measurements

Air compressor units in many industries do not have inlet piping because the absence of inlet piping helps to prevent piping pressure losses. Therefore, measurements of the properties of air at the inlet should be done in the region of the air intake into the compressor. When taking inlet measurements, it is important to ensure that interference of weather, direct sunlight, and

temperature fluctuations are prevented. Measurements of inlet temperature, ambient pressure, and relative humidity should be taken at the inlet of the compressor unit. In addition, power to the compressor should be measured at the input supply to the compressor unit. (ASME PTC 13-2018, 2019.)

3.3.2 Outlet Measurements

Outlet temperature, outlet pressure and mass flow should be measured at the outlet of the compressor unit. In this chapter, four alternative designs for measuring the compressor unit outlet temperature, outlet pressure and outlet mass flow using three different flowmeter options are discussed.

3.3.2.1 Measurement setup using Cone meter

According to ASME PTC 13-2018 (2019), measurement locations of the outlet pressure should be before the outlet temperature and subsequently before the flow measurement device. The pressure measurement locations should be at a minimum distance of 0.305 m from the compressor unit discharge. Four pressure measurement locations are distanced at increments of 90º from each other around the circumference of the pipe. The measurement taps for pressure instruments can be in a manifold (tied together) in order to find the average reading. The pressure taps should be indexed 45º at a minimum of 0.203 m distance from the adjacent four temperature instruments. There should be insulation of the pipe from the compressor unit discharge flange to the temperature and flowmeter measuring regions. The temperature measurement instruments should be immersed at least 30% of the pipe radius as illustrated in Figure 8, where r is the radius.

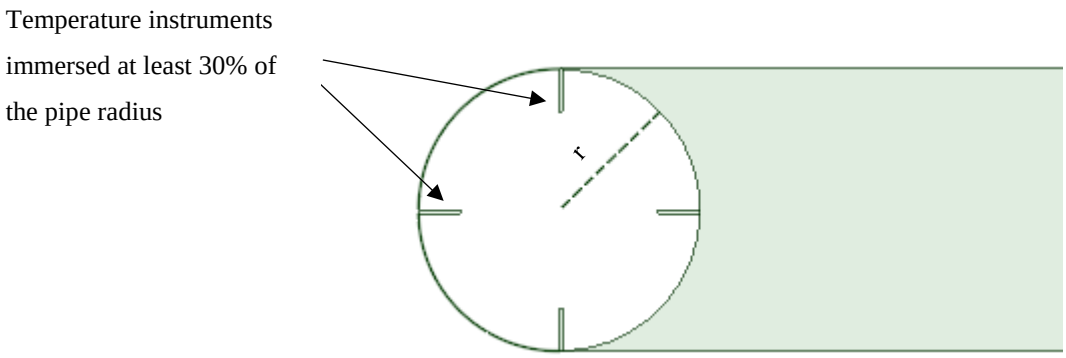

Figure 8. Immersion lengths of the temperature measurement instruments

According to the ISO 5167-5 (2016) (Measurement of fluid flow by means of pressure differential devices inserted in circular cross-section conduits running full – Part 5: Cone meters), the upstream length of the cone meter is measured from the plane of the centerline of the upstream tapping. The downstream length is measured from the plane of the beta edge. In order to optimize the use of cone meter technology, the preceding disturbances and the upstream lengths were compared as shown in Table 2 in order to recommend a suitable piping configuration. In Table 2, D refers to the diameter of the pipe.

Table 2. The minimum upstream and downstream lengths according to ISO 5167-5 (2016)

Disturbance	Beta ratio	Upstream length	Downstream length
Single 90º bend	$0.45 \leq \beta < 0.6$	3D	2D
	$0.6 \leq \beta \leq 0.75$	6D	2D
Two 90º bends	$0.45 \leq \beta < 0.6$	3D	2D
	$0.6 \leq \beta \leq 0.75$	6D	2D
Concentric expander with 0.75D to 1D	All	3D (0.5% uncertainty is added)	2D
Partially closed valves	All	10D	2D

Based on the considerations in Table 2, a design of the piping configuration was made and is shown in Figure 9. The Figure 9 is a schematic diagram of the piping configuration. In accordance with ISO 5167-5 (2016), the flow direction is from the compressor unit outlet flange and there should be a minimum of 0.35 m distance from the outlet flange to the centerline of the pressure taps which are 0.25 m from the centerline of the temperature taps. There are four temperature and pressure taps, and the cone meter should have a beta angle of $0.45 \leq \beta < 0.6$ based on the design recommended in Figure 9.

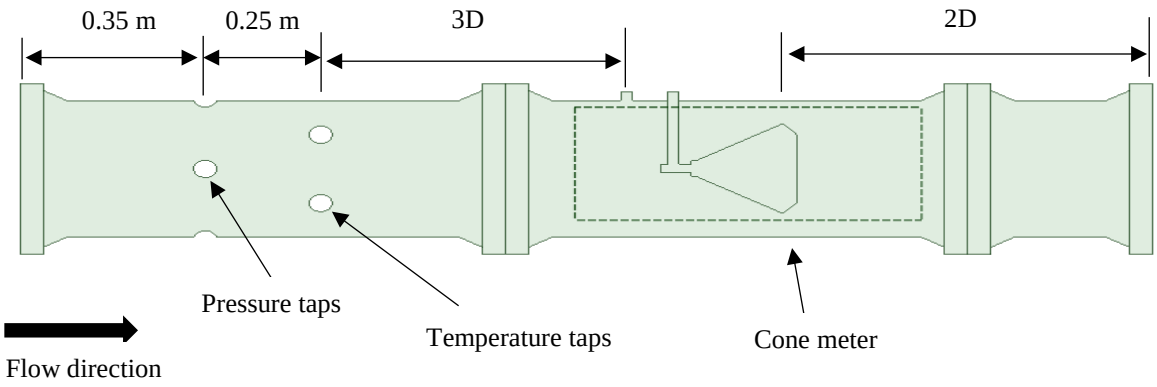

Figure 9. Compressor outlet piping configuration when using a cone meter

There are very limited or no cases where the disturbances from partially closed valves or concentric expanders are found, therefore, they are not taken into account. To optimize cone meter technology when space requirements, disturbances, and pressure drop are considered, the cone meter chosen should be of $0.45 \leq \beta < 0.6$. Also, in industries where measurements are done, there are space limitations and this was considered when designing the outlet piping. It is thus advantageous that this design has short upstream and downstream lengths.

3.3.2.2 Measurement setup using Ultrasonic meter

There are different measurement piping configurations that can be used for ultrasonic meter (USM) based on whether there is a unidirectional flow, bidirectional flow, or need for flow conditioner. A conservative design for a unidirectional flow with flow conditioner requires a minimum of 20D upstream length of the USM inlet flange, and a minimum of 2D-5D downstream length from the USM discharge flange to the centerline of the temperature wells. However, when flow conditioners are not used for a unidirectional flow in this case, the design in Figure 10 should be followed. In the most compact of designs for the outlet piping configuration, there should be a minimum upstream length of 10D from the compressor outlet flange to the USM inlet flange as shown in Figure 10. The temperature measurement locations should be located 2-5D from the USM outlet flange. The first temperature measurement location should be at least 0.15 m or 2D from the flange (whichever one is larger) but no more than 5D from the USM outlet flange face. The temperature instruments should be immersed at least 30% of the pipe radius. (AGA Report No. 9, 2017.)

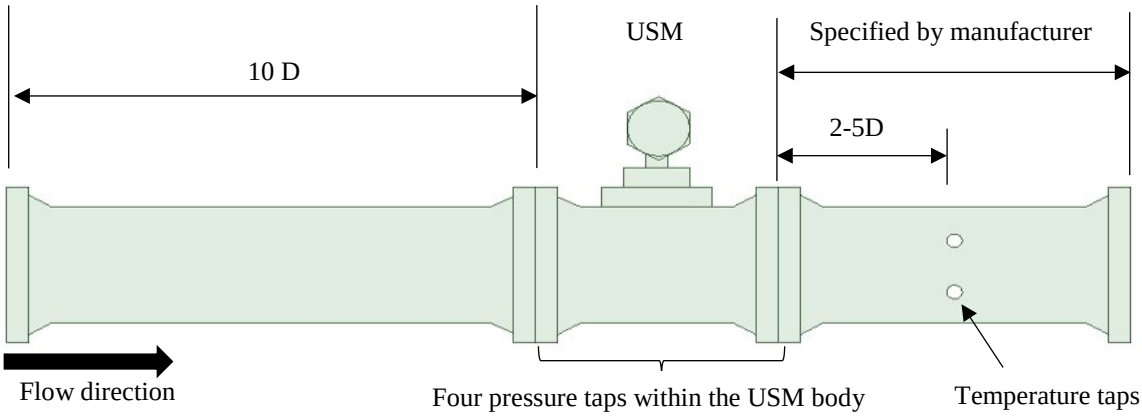

Figure 10. Compressor outlet piping configuration when using an USM

As shown in Figure 10, the configuration designed in this thesis follows the ASME PTC 13-2018 (2019) standard where the four temperature measurement locations are all around the pipe circumference. In the design, there are four pressure measurement locations in accordance with ASME PTC 13-2018 (2019). According to AGA Report 9 (Measurement of Gas by Multipath Ultrasonic Meters), the holes of pressure taps should be located within the body of the ultrasonic meter. Each hole should be between 3.2 – 9.5 mm nominal inside diameter over a length of at least 2.5 times the tapping diameter. Their positions should be agreed with the USM manufacturer so that the position does not interfere with the ultrasonic path because the manufacturer determines the location of the pressure instruments based on the paths. (AGA Report No. 9, 2017.)

The use of ultrasonic meter in flow measurement is beneficial because there is minimal pressure drop and they have high accuracy. It is also suitable for a wide range of pipe diameter, but the error may increase as the flow diameter increases. However, long inlet and outlet lengths are needed which may be a limitation when conducting the measurements in industries. (AGA Report No. 9, 2017.)

3.3.2.3 Measurement setup using Coriolis meter

In a Coriolis meter, a phenomenon known as flow pressure effect occurs if the operating pressure changes; which leads to bias. This flow pressure effect in Coriolis flowmeter results from flow tube stiffening due to the pressure increase. This will thus affect the Coriolis force because the Coriolis effect is more effective at lower pressures. The Coriolis effect decreases

with increasing pressure at a particular mass flow rate and vice versa. However, for the pressure effect to have a considerable error of 0.1% in mass flow rate, there needs to be a pressure increase of about 7 bar. This is because the pressure effect has a range of -0.001% to 0% per 0.069 bar (Stappert, 2007). The pressure effect can only be a considerable source of error at high pressures usually more than 34 bar. Moreover, the Coriolis pressure effect on performance is more evident in liquids than in gas and air applications. Therefore, in compressed gas applications, this would not pose a problem since the operating pressure is 6-7 bar. This error problem can alternatively be prevented by calibrating the flowmeter at the operating pressure. (Stappert, 2007; Calame, 2013)

Nonetheless, any error problem related to the Coriolis pressure effect would be prevented altogether by installing pressure measurements since outlet pressure measurement is still needed in efficiency calculations. Therefore, outlet pressure measurement locations would be installed in the piping configuration to serve both purposes of measuring the outlet pressure and to remove possible errors due to Coriolis effect through flow pressure compensation. The pressure sensor should be installed upstream and close to the Coriolis meter. The pipe containing the pressure transducers should also be well insulated.

Although temperature measurement is not needed for reference volume and energy calculations according to AGA Report No. 9 (Measurement of Natural Gas by Coriolis meter), installation of temperature measurement instrument is recommended. In the case that there are temperature measurement locations, the temperature taps should be located upstream in order to validate the temperature measured by the Coriolis sensor and remove the necessity of correction for the Joule-Thomson effect at high pressure drops. In the case that there are no temperature measurement locations, routine flowmeter verification should be done to ascertain that the temperature readings from the Coriolis flowmeter are within the tolerance indicated by the manufacturer. Also, calibration at operating temperatures will help to prevent bias in the temperature measurements (AGA Report No. 11, 2013.) In this application, there are no extreme and high pressure drops, therefore, temperature measurements may be removed from the design to make the design more compact.

Therefore, two designs were made when the Coriolis meter is used as the instrument for flow measurement. The first design in Figure 11 does not have outlet temperature measurement

(it has only four pressure measurement locations). The second design in Figure 12 has four temperature and four pressure measurements on the upstream of the Coriolis meter. The temperature instruments are immersed at least 30% of the pipe radius.

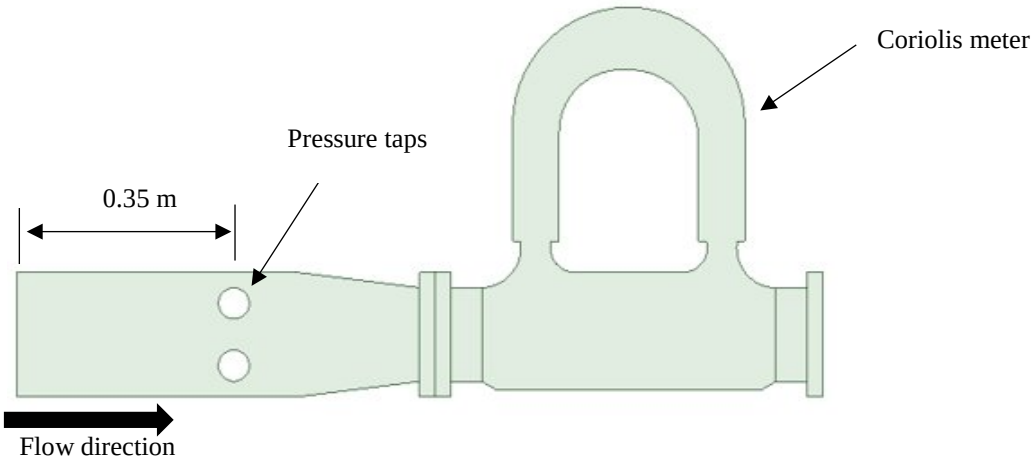

Figure 11. Coriolis meter with only pressure measurement upstream (no temperature measurements)

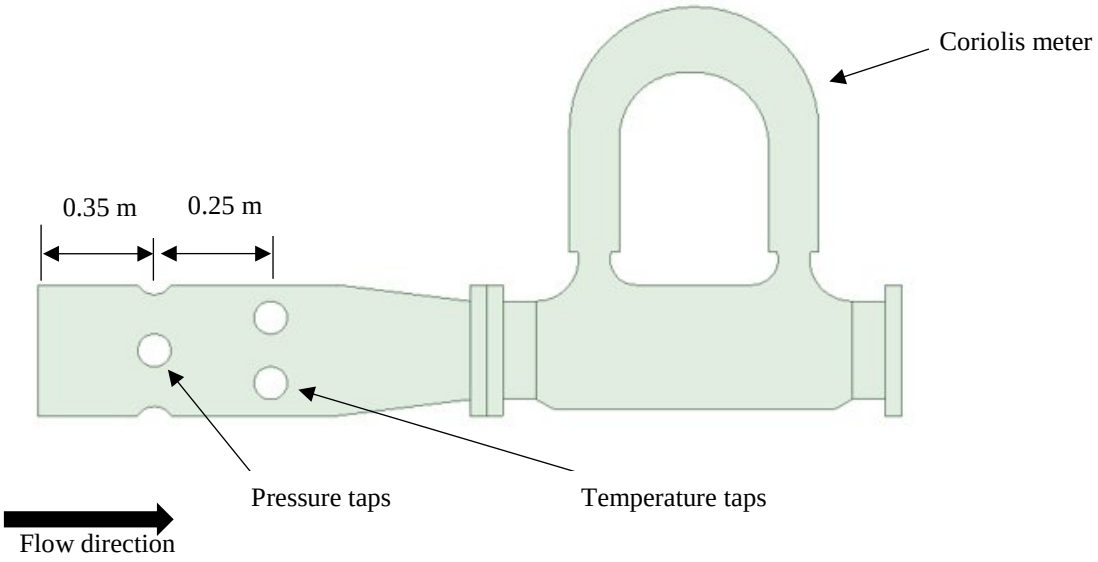

Figure 12. Coriolis meter with pressure and temperature measurements upstream

The design has advantages in that mass flow, density and temperature can be measured simultaneously. There is no necessity for having downstream lengths although pipe support may be needed. Coriolis meters are also advantageous because of their high accuracy.

3.3.3 Comparison of the measurement setups

The different measurement setups for the compressor outlet have different advantages and disadvantages that need to be considered in order to choose the most suitable design. Some of the relevant differences are summarized in Table 3.

Table 3. Comparison of flowmeter options for compressor outlet measurements

DP Cone meter	Coriolis meter	Ultrasonic meter
Advantages - Short upstream and downstream meter runs - Familiarity with the technology - Lower costs	Advantages - No downstream lengths needed - Simultaneous mass flow, density, and temperature measurements - The most compact of the three designs, therefore, easy to install - Accuracy up to ±0.5% of flow (Tricor, n.d.)	Advantages - Low pressure drop - Suitable for a wide range of pipe diameter - Flow calibrated accuracy of ±0.1-0.5% of flow (Emerson Electric, 2019; Transus Instruments, n.d.)
Disadvantages - Higher pressure drop - Accuracy of up to ±0.5% of flow reading and 1% of full scale (McCrometer, 2017)	Disadvantages - Pipe support may be needed - Possible need for expanders or reducers - Relatively higher costs	Disadvantages - Long upstream and downstream meter runs - Relatively higher costs - Difficulty in installation where there is limited space.

Based on the comparisons, trade-offs can be made before choosing the technology to use. Tentatively, the Coriolis meter appears to be the most beneficial and suitable because of the accuracy level, its compactness, and direct mass flow measurement. Nonetheless, further comparisons of the flowmeter options are done in the measurement uncertainty estimation in Chapter 5 in order to finally recommend the best available option.

4 DETERMINATION OF ISENTROPIC EFFICIENCY AND THE CALCULATION PROCESS

4.1 Ideal model of the two-stage dry screw compressor

Many industries using air compressors have multistage compressors, with intercooling and aftercooling. Dryers can be used to dry the compressed wet air before the air is used. From the compressor unit in Figure 13, air goes in from the compressor inlet, passes through the air filter, and into the first stage screw element. The first compression takes place and the pressure and temperature of air increases due to compression. The air then goes into the intercooler, which is a heat exchanger that cools down the air to low temperature. The pressure losses in the intercooler is less than 0.07 bar and the moisture in the air due to cooling condenses in the condensate water separator (ASME PTC 10-1997, 1998).

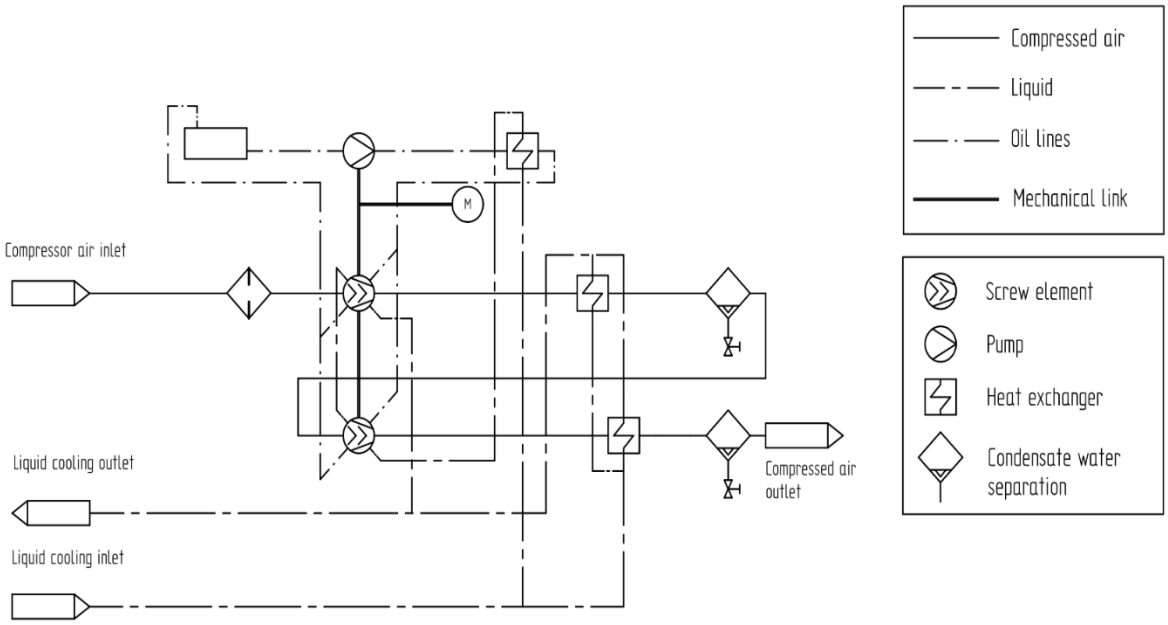

Figure 13. P&ID of a typical two-stage compressor unit

The higher pressure-lower temperature air then moves into the second stage screw element where further compression takes place. This increases the air temperature and further increases the pressure of air. The aftercooler cools the air down again and there is the removal of the condensate at the aftercooling. The pressure losses in the aftercooler is about 0.07 bar (ASME PTC 10-2018, 2019). At the condensate water separation, there are losses in the mass flow due to condensate removal. In some compressor unit designs, there is a dryer between the aftercooler and the compressed air outlet. The pressure losses in the dryer is

about 0.09 bar (Atlas Copco, 2019). The dryer removes moisture from the air before it is used. In some compressor unit designs, the dryer present before the compressed air outlet is used to dry the high-temperature air which directly leaves the second stage compressor without going through the aftercooler. This is due to the partial extraction of air between the second stage and the aftercooler. The compressor unit also shows the liquid lines used for cooling of the air, and the oil that cools the bearings and gears.

Intercooling reduces the power that is consumed by the second stage compressor by removing heat from the air. In most two-stage compressors, there is incomplete intercooling whereby the entry temperature into the second stage screw compressor is not equal to the inlet temperature of the first stage screw compressor. The effect of cooling thus subsequently helps to increase the compressor efficiency. To calculate the isentropic efficiency of the compressor, some simplifications and assumptions were made as follows.

- Inlet and outlet temperature of the cooling liquid were not measured. The liquid cooling inlet temperature was not used as an input value because the mass flow of the liquid supply was not known.
- Oil cooling was not considered in the calculation process because of the unavailability of data on the type of oil used and the mass flow of the oil. Therefore, the mass flow of oil was not measured in the measurement setup because of the simplified system.
- When a dryer is present, the partial extraction of air before the aftercooler was not considered since the quantity extracted was not known. This only slightly affected the division of condensate removal at the aftercooling and dryer. This is because it increases the cooling needed in the dryer for the air extracted to the dryer from the second stage screw compressor. Therefore, it does not affect the total amount of condensation in the system.
- When a dryer is present, the dryer was considered as a heat exchanger in the calculation process. Therefore, the amount of condensation in the dryer was calculated from the humidity ratios at the inlet and outlet of the dryer.

Based on the above simplifications, three measurement scenarios were examined;
Measurement scenario 1 – no temperature and pressure measurements inside the compressor unit, only the speed is measured
Measurement scenario 2 – measurement of speed and the second stage outlet temperature
Measurement scenario 3 – several measurements inside the compressor unit

4.2 Measurement scenario 1

This is the first scenario considered to determine if the compressor isentropic efficiency can be determined without making temperature and pressure measurements inside the compressor unit. This option was considered because in many industries using dry screw compressors, there can be restrictions from the compressor owner to conducting measurements inside the compressor unit. The measurement setup with the compressor unit measurements are shown in Figure 14.

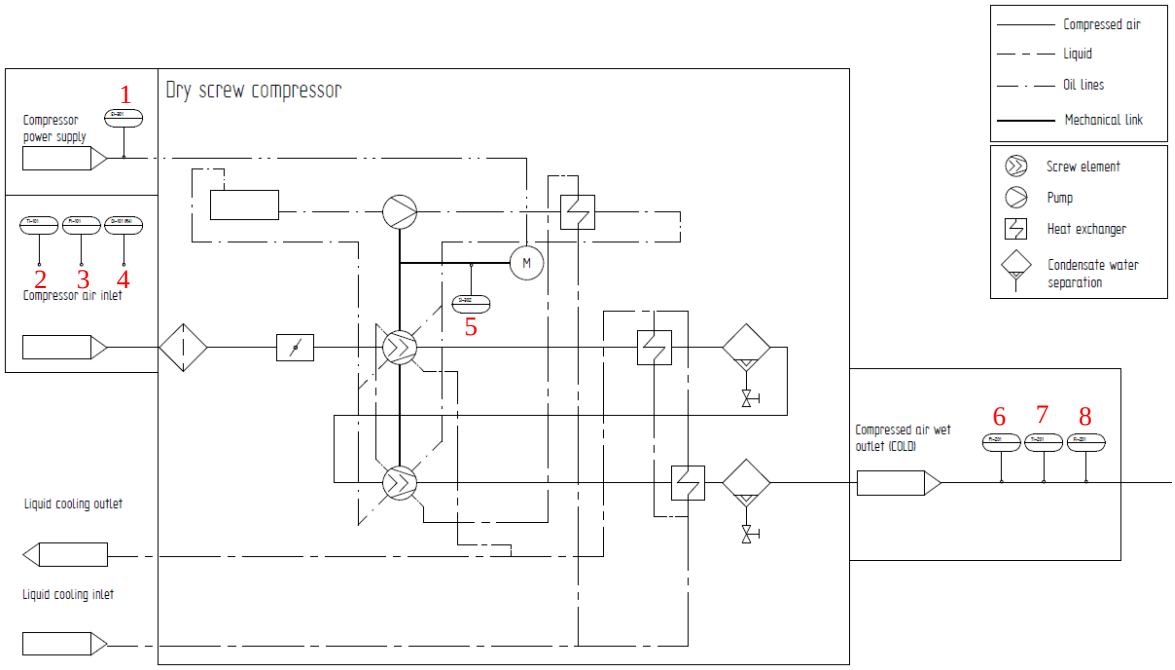

1-Power input	2-Ambient temperature	3-Ambient pressure	4-Relative humidity
5-Speed	6-Outlet pressure	7-Outlet temperature	8-Outlet flow rate

Figure 14.The required measurements for measurement scenario 1

Isentropic compression is an ideal thermodynamic process that is adiabatic and reversible. It means there is no heat transfer. Isentropic efficiency is thus used in determining the compressor performance in this thesis. A Microsoft excel tool was made which shows all the

calculation steps for determining the compressor efficiency and the calculated results. The process of calculating the compressor isentropic efficiency for measurement scenario 1 is in accordance with the following four calculation steps.

STEP 1: Compression and cooling calculations
STEP 2: Condensation and mass flow calculations
STEP 3: Isentropic efficiency calculation
STEP 4: Calculation back to reference conditions

4.2.1 STEP 1: Compression and cooling calculations

The first step of the calculation process requires the calculation of the thermodynamic characteristics over the compressor unit without internal measurements. Here, the partial pressure of vapor is calculated and it is dependent on the relative humidity and pressure of saturated vapor. The pressure of dry air is also calculated from ambient pressure and partial pressure of vapor. Then, the humidity ratio at the compressor unit inlet and compressor unit outlet, specific gas constant of the mixture, molecular weight of the water-air mixture, molar specific heat of the mixture, isentropic exponent, and the pressure ratio was calculated. For real gases, the isentropic exponent is the ratio of specific heat of the mixture. The pressure ratio is the ratio of outlet pressure to inlet pressure. In scenario 1, it was assumed that the compressor ratio is equally divided between the two stages. Therefore, the pressure ratio is calculated using Equation (1).

$$\pi = \sqrt{\frac{p_2}{p_1}}\,. \tag{1}$$

Where $p_1$is the pressure at the inlet of the compressor unit and p_2 is the pressure at the outlet of the compressor unit.

The humidity ratio (HR) is the ratio of air mass to vapor mass in the mixture. The humidity ratio (HR) was calculated at the compressor unit inlet and at the outlet of the compressor unit. At both locations, HR was calculated using the Equation (2) (ASME PTC 10-1997; 1998.)

$$HR = \frac{R_{\mathrm{da}}}{R_{\mathrm{vp}}} \cdot \frac{p_{\mathrm{vp}}}{p_{\mathrm{da}}}\,, \tag{2}$$

where the constants R_{da} and R_{vp} are the gas constants of dry air and vapor respectively. p_{vp} and p_{da} are the pressures of vapor and dry air respectively.

The results of the humidity ratio (HR) were used to calculate the flow rate at the inlet of the compressor unit. The results of the specific gas constant of the mixture (R), isentropic exponent (κ), and pressure ratio (π) are used in step 3 for efficiency calculations. (ASME PTC 13-2018, 2019)

4.2.2 STEP 2: Condensation and mass flow calculations

Step 2 is in accordance with ASME PTC 10-1997 (1998). The measured mass flow at the outlet of the compressor unit, humidity ratio at the inlet and at the outlet of the compressor unit are needed for calculations. Equation (3) was used to determine the mass flow rate into the compressor unit. The results were then used for calculations in step 3. (ASME PTC 10-1997, 1998.)

$$q_{\mathrm{m},1} = q_{\mathrm{m},2} \cdot \left(\frac{1+HR_1}{1+HR_2}\right), \tag{3}$$

where $q_{\mathrm{m},1}$ is the mass flow at the compressor unit inlet, $q_{\mathrm{m},2}$ is the mass flow at the compressor unit outlet, HR_1 is the humidity ratio at the compressor unit inlet, HR_2 is the humidity ratio at the compressor unit outlet.

The mass flow loss at the compressor stages was due to cooling and condensation, which subsequently leads to the removal of the condensate water. Other calculations that were done in step 2 include the determination of the ratio of the condensate to dry air, mass flow of the dry air and the mass flow of the condensate.

4.2.3 STEP 3: Isentropic efficiency calculation

The isentropic efficiency was determined using the calculation results from steps 1 and 2. The isentropic efficiency is calculated as a ratio of the isentropic power ($\dot{W}_{\mathrm{is}}$) to the actual power ($\dot{W}_{\mathrm{act}}$). Equation (4) is used for calculating isentropic efficiency. (Brasz, 2006.)

$$\eta_{\mathrm{is}} = \frac{Ideal\ input\ power}{Actual\ input\ power} = \frac{\dot{W}_{\mathrm{is}}}{\dot{W}_{\mathrm{act}}} = \frac{\frac{\kappa}{\kappa-1} q_{\mathrm{m},1} R T_1 (\pi^{\frac{\kappa-1}{\kappa}} - 1)}{\dot{W}_{\mathrm{act}}}. \tag{4}$$

where κ is the isentropic exponent, $q_{\mathrm{m},1}$ is the compressor unit inlet mass flow, R is the specific gas constant of the mixture, T_1 is the compressor unit inlet temperature, π is the pressure ratio, $\dot{W}_{\mathrm{act}}$ is the actual input power (can be determined by speed and torque measurement using a power analyzer).

In measurement scenario 1, it is assumed that the actual input power measured is equally divided between the two compressor stages. This is because Equation (4) takes the whole compressor unit as one compressor. Therefore, the actual input power measurement is for both compression stages while the ideal input power calculated takes the compressor as a single stage. Thus, the actual input power $\dot{W}_{\mathrm{act}}$ is recalculated using Equation (5).

$$\dot{W}_{\mathrm{act}} = \frac{\dot{W}_{\mathrm{act,measured}}}{2} \tag{5}$$

If the assumption that the actual input power is equally divided between both stages is not made, the isentropic efficiency will give wrong results which will be lower than the expected isentropic efficiency.

4.2.4 STEP 4: Calculation back to reference conditions

When conducting performance tests, calculation back to reference conditions needs to be done using the reference conditions; 101.325 kPa, 20 °C, and 0% for the pressure, temperature, and relative humidity respectively. The mass flow, rotational speed, and power were calculated back to reference conditions using Equations (6), (7) and (8) respectively. (Turunen-Saaresti, 2004.)

$$q_{\mathrm{m,ref}} = q_m \cdot \frac{p_{1,\mathrm{ref}}}{p_1} \sqrt{\frac{T_1 R}{T_{1,\mathrm{ref}} R_{\mathrm{ref}}}}, \tag{6}$$

where ref are the reference conditions; and those without ref as a subscript are at test conditions. The specific gas constant at reference conditions was calculated from the relative humidity at reference conditions.

$$N_{\mathrm{ref}} = N \sqrt{\frac{T_{1,\mathrm{ref}} R_{\mathrm{ref}}}{T_1 R}}, \tag{7}$$

where N is the rotational speed

The calculation result of rotational speed at reference conditions from Equation (7) was used in calculating the power at reference conditions as shown in Equation (8). (ISO 1217, 2009.)

$$P_{\mathrm{ref}} = \left(\frac{N_{\mathrm{ref}}}{N}\right)^2 \cdot P \ , \tag{8}$$

where P is the measured power, the term $\left(\frac{N_{\mathrm{ref}}}{N}\right)^2$ is the correction factor for speed,

The advantage of using measurement scenario 1 is that the isentropic efficiency can be estimated across the whole compressor unit without taking internal compressor unit measurements. However, the disadvantages with measurement scenario 1 are that it is difficult to evaluate the effect of cooling inside the compressor unit, and some estimations and assumptions were made in order to determine the isentropic efficiency. It was assumed that the pressure ratio is equally divided between both compressor stages. It was also assumed that the input power into the first stage and the second stage is the same. In many cases, the power to the first stage can be more than the power to the second stage due to the effect of intercooling. These assumptions thus question whether the assumptions made are enough or within acceptable limits to properly estimate the performance of the compressor.

4.3 Measurement scenario 2

Since the first measurement scenario has uncertainties due to the inability to examine cooling effects, a second scenario was considered where the outlet temperature of the second stage can be measured. This scenario was a step further to check the effects of aftercooling when estimating compressor efficiency. Measurement of the second stage outlet temperature helps to have a view of the aftercooling effect by plotting an enthalpy-entropy (h-s) diagram. In Figure 15, measurement of temperature at the outlet of the second stage compressor was included. Figure 15 shows the internal compressor unit measurements and the external measurements for the measurement scenario 2.

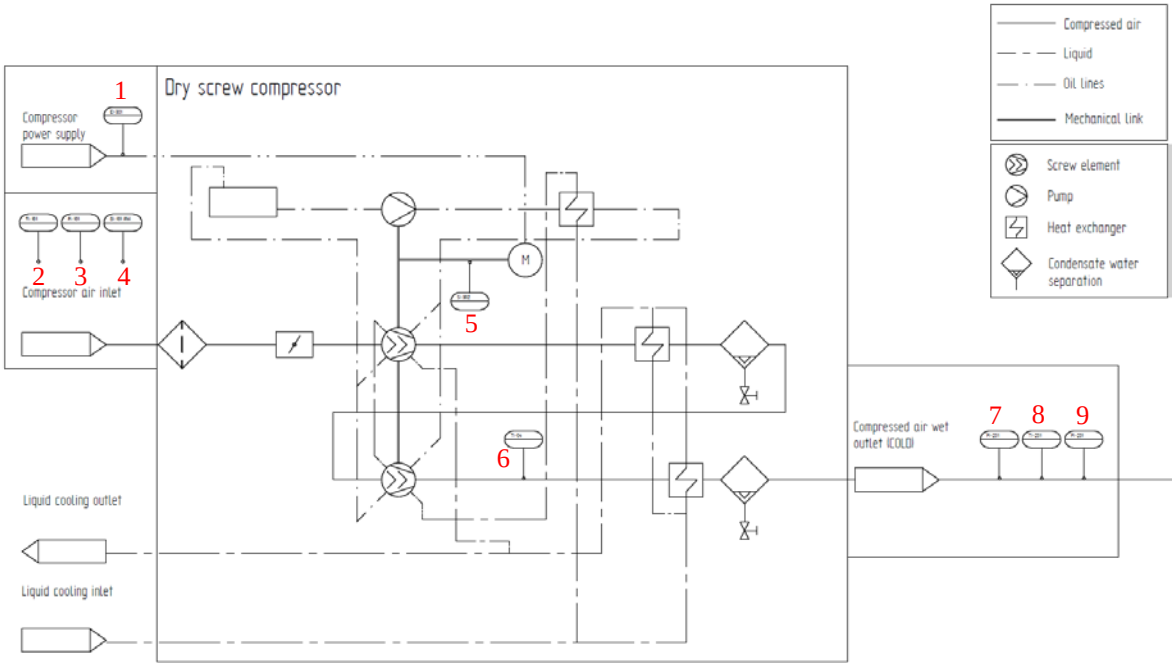

1-Power input	2-Ambient temperature	3-Ambient pressure
4-Relative humidity	5-Speed	6-Second stage outlet temperature
7-Compressor unit outlet pressure	8-Compressor unit outlet temperature	
9-Compressor unit outlet flow rate		

Figure 15. The required measurements for measurement scenario 2

In this measurement scenario 2, there are still many unknowns and uncertainties. Properties that were not taken into consideration include the intercooling that affects the second stage inlet temperature, which subsequently reduces the power used by the second stage. Incomplete intercooling is common in two-stage dry screw compressors, which reflects on the second stage inlet temperature as the air may be cooled to a temperature different from the inlet temperature of the first stage. In a two-stage compressor, there are uncertainties due to the assumption of equally dividing the pressure ratio between both compression stages. Also, there are uncertainties with assuming that each stage consumes the same amount of power.

4.4 Measurement scenario 3

Measurement scenario 3 involves a more detailed measurement system whereby there are several measurements of air temperature and pressure inside the compressor unit. This is to help reduce the number of unknowns and ensure better efficiency analysis. Liquid inlet temperature was not used as an input value but the effects of cooling due to intercooling are accounted for in the efficiency calculation results as it affects the inlet temperature of the

second stage. The conditions of the air at the outlet of the first stage and the second stage are the same as the inlet conditions of the intercooler and the aftercooler respectively. Therefore, the pressure at the second stage inlet is assumed to be equal to the pressure at the first stage outlet.

Also, the pressure at the compressed air outlet is equal to the pressure at the second stage outlet due to the neglect of the minimal pressure losses in the aftercooler. The locations of measurements needed inside the compressor unit and the external measurements are shown in Figure 16 and Figure17. Figure 16 is without a dryer and the compressor unit produces compressed wet air. Figure 17 has a dryer and the compressor unit produces compressed dry air. The difference between the measurement setups is that the temperature and pressure at the outlet of the aftercooler are measured when there is a dryer in the setup. Measurement of the temperature at point A and pressure at point B in Figure 17 helps to account for any pressure losses in the dryer or piping losses.

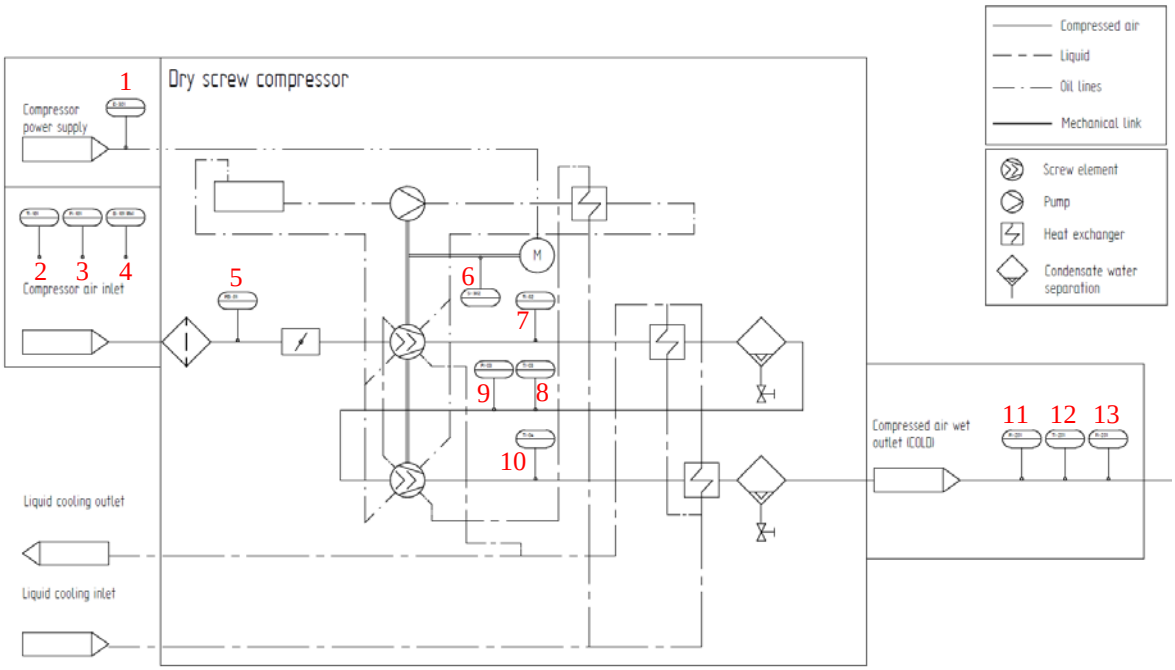

Figure 16. The required measurements for measurement scenario 3 without a dryer (wet air)

1-Power input	2-Ambient temperature	3-Ambient pressure
4-Relative humidity	5-Pressure difference	6-Speed
7-First stage outlet temperature	8-Second stage inlet temperature	9-Second stage inlet pressure
10-Second stage outlet temperature	11-Compressor unit outlet pressure	
12-Compressor unit outlet temperature	13-Compressor unit outlet flow rate	
A-Aftercooler outlet temperature	B-Aftercooler outlet pressure	

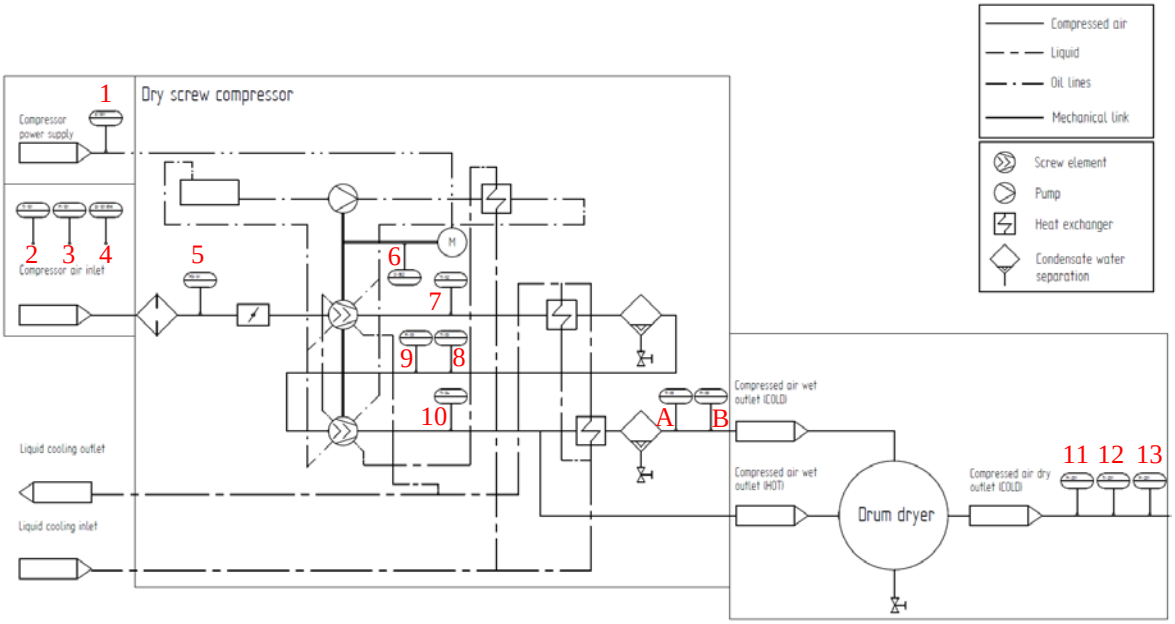

Figure 17. The required measurements for measurement scenario 3 with a dryer (dry air)

To have better results and analysis in the efficiency determination, pressure and temperature measurements inside the compressor unit are needed. In measurement scenario 3, the inter-cooling is accounted for through the measurement of the second stage inlet temperature. When a dryer is present, two more measurements are made inside the compressor unit; the temperature and pressure at the outlet of the aftercooler. According to ASME PTC 10-1997 (1998) and ASME PTC 13-2018 (2019), the cooling inlet and outlet temperatures, and flow rates of the cooling streams should also be measured during the performance test. However, due to the inability of having detailed measurement locations at the liquid cooling lines, the calculation does not utilize cooling temperature as an input variable in order to evaluate its effect on efficiency.

When determining the compressor performance in measurement scenario 3, the steps used were in accordance with the steps mentioned in measurement scenario 1. However, there were some differences because the internal compressor unit measurements in scenario 3 allow for making calculations for each stage separately.

In step 1 (compression and cooling calculations), there was calculation of the thermodynamic characteristics for each stage of the compression as done in scenario 1. However, when calculating the pressure ratio in scenario 3, no assumptions were made that the pressure ratio was equally divided between the two stages because the pressure at the inlets and outlets of both stages was measured. Therefore, the pressure ratio in measurement scenario 3 was calculated using Equation (9).

$$\pi = \frac{p_2}{p_1}\,. \tag{9}$$

where $p_1$is the pressure at the inlet of the compressor stage and p_2 is the pressure at the outlet of the compressor stage. The pressure ratio was calculated for the first stage and for the second stage.

Also, the humidity ratio (HR) was calculated at four locations in the compressor unit; the first stage inlet, the second stage inlet, the outlet of the aftercooler, and at the outlet of the dryer. The HR at the four locations gives information on the mass flow into each stage, the ratio of condensate to dry air, flow rate of dry air, and flow rate of condensate at each stage. For condensation to occur at the intercooler and aftercooler, saturated humidity ratio must be less than the humidity ratio at the cooler inlets. If the saturated HR is greater than the inlet

HR, then condensation does not occur. The dryer was also taken as a heat exchanger and the HR at its outlet was calculated. The calculations are in accordance with the method outlined in ASME PTC 13-2018 (2019) and ASME PTC 10-1997 (1998) standards.

In step 2 (condensation and mass flow calculations), the measured mass flow at the outlet of the compressor unit and the humidity ratios are needed for calculations. The calculation was done in reverse flow direction since the mass flow measured in test conditions is at the outlet of the compressor unit. Therefore, it was possible to first calculate the mass flow at the dryer inlet, then the mass flow at the second stage inlet, and then finally the mass flow at the first stage inlet. Equation (10) was used to determine the mass flow rates accordingly at the first stage, second stage, and dryer. The results were then used in step 3. (ASME PTC 10-1997, 1998.)

$$q_{\mathrm{m},1} = q_{\mathrm{m},2} \cdot \left(\frac{1+HR_1}{1+HR_2}\right), \tag{10}$$

where $q_{\mathrm{m},1}$ is the mass flow at the inlet, $q_{\mathrm{m},2}$ is the mass flow at the outlet, HR_1 is the humidity ratio at the inlet, HR_2 is the humidity ratio at the outlet. This calculation were done for the first stage, second stage, and the dryer.

The mass flow loss at the compressor stages and the dryer were due to cooling and condensation, which subsequently leads to the removal of the condensate water. Other calculations that were done in step 2 include the ratio of the condensate to dry air, mass flow of the dry air, and the mass flow of the condensate. In the results, the mass flow rate of the dry air should remain constant but the mass flow rate of the condensate should differ.

In step 3, the isentropic efficiency formula was different compared to measurement scenarios 1 and 2 because assumptions were not made with the ideal input power and the actual input power. The ideal input power was calculated separately for the first stage and second stage, and then summed together to get the total ideal input power. There was no assumption that the actual input power was equally divided by both stages because the actual input power measured is the total power that goes into the whole compressor unit. Therefore, isentropic efficiency was calculated using Equation (11).

$$\eta_{\text{is}} = \frac{Ideal\ input\ power}{Actual\ input\ power} = \frac{\dot{W}_{\text{is,total}}}{\dot{W}_{\text{act}}} = \frac{\dot{W}_{\text{is,first}} + \dot{W}_{\text{is,second}}}{\dot{W}_{\text{act}}}$$

$$= \frac{\left[\frac{\kappa}{\kappa-1} q_{\text{m},1} R T_1 \left(\pi^{\frac{\kappa-1}{\kappa}} - 1\right)\right]_{first} + \left[\frac{\kappa}{\kappa-1} q_{\text{m},1} R T_1 \left(\pi^{\frac{\kappa-1}{\kappa}} - 1\right)\right]_{second}}{\dot{W}_{\text{act}}}, \quad (11)$$

where $\dot{W}_{\text{is,total}}$ is the ideal input power, $\dot{W}_{\text{act}}$ is the actual input power, κ is the isentropic exponent, $q_{\text{m},1}$ is the inlet mass flow, R is the specific gas constant of the mixture, T_1 is the inlet temperature, π is the pressure ratio, subscripts $first$ and $second$ are for the first stage and second stage respectively.

The step 4 (calculation back to reference conditions) follows the same process as used in scenario 1.

Advantages of using measurement scenario 3 is that the mass flow and .the intercooling effect are considered in the calculation process. The assumptions related to pressure ratio, actual input power, ideal input power were also eliminated because calculations were done for each stage

4.5 Enthalpy-Entropy chart

The purpose of the enthalpy-entropy chart (h-s chart) is to show the effect of liquid cooling in the process. It helps to visualize the effect of intercooling and aftercooling in the compressor unit. Standard conditions of air were used as the first stage inlet conditions. In the technical specification of some VSD oil-free screw compressors from Atlas Copco, the working pressures were 4 bar minimum, 7.5 bar effective, and 10.4 bar maximum (Atlas Copco, 2018). The effective working pressure of 7.5 bar was used. It was assumed that the pressure ratio is equally divided between both compression stages which puts the pressure ratio at each stage below the maximum of 3.5 for dry screw compressors (Kovacevic et al, 2006). The working temperatures that were used as operation values were estimated. The summary of estimated operation values in Table 4 is used to plot the h-s chart in Figure 18.

Table 4. Estimated values used for plotting the h-s graph

Points in the compressor unit	Operation values
Compressor unit inlet	1 bar, 20℃
First stage outlet/Intercooler inlet	2.7 bar, 160℃
Second stage inlet/Intercooler outlet	2.7 bar, 30℃
Second stage outlet/Aftercooler inlet	7.5 bar, 140℃
Aftercooler outlet	7.5 bar, 30℃

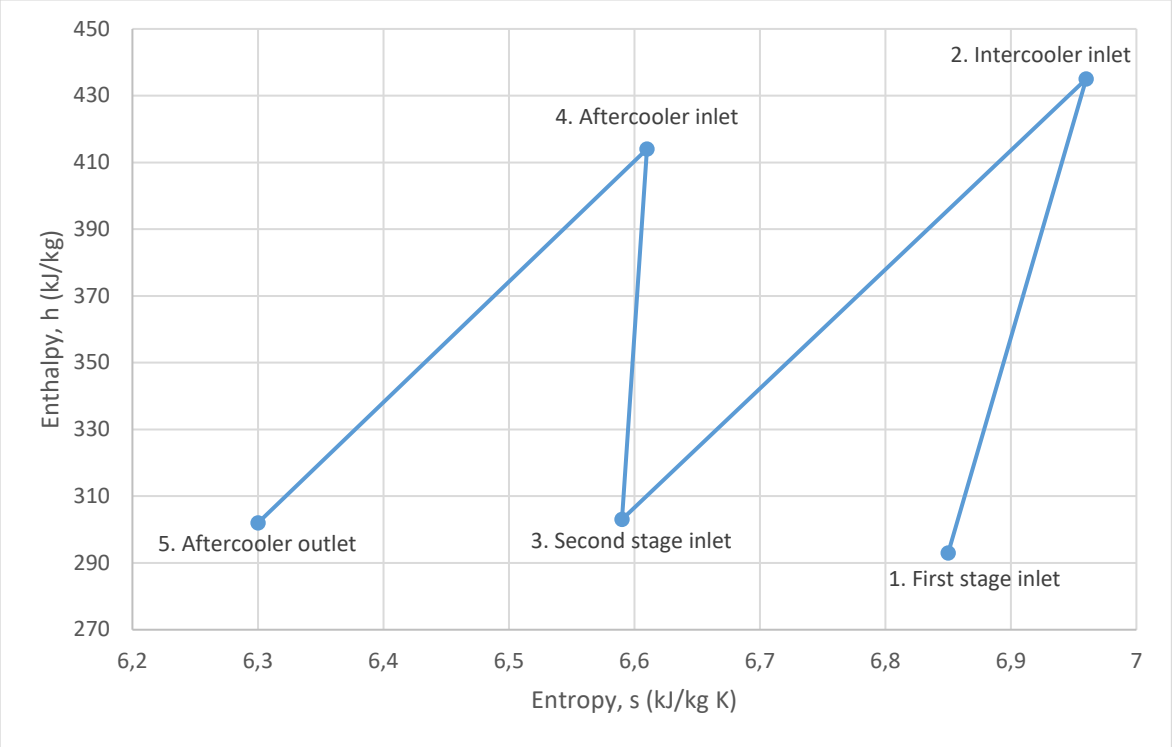

Figure 18. Enthalpy-Entropy chart of different points in the compressor unit

The h-s chart in Figure 18 shows that enthalpy increases from the first stage inlet to the outlet of the first stage due to compression. The entropy also increases during compression. As enthalpy is a function of temperature, the enthalpy and the entropy decreases when air is cooled at the intercooler. The air at the outlet of the intercooler is then at low temperature,

lower enthalpy, and lower entropy compared to the inlet of the intercooler. The second compression takes place and increases the enthalpy and entropy due to an increase in the pressure. The aftercooler cools the air down which reduces the enthalpy and temperature. The air at the aftercooler outlet is then at low temperature and high pressure. Figure 18 thus shows that compression increases enthalpy and entropy while cooling decreases the enthalpy and entropy. In Figure 18, there is more entropy change from the first stage inlet to intercooler inlet compared to the second stage inlet to aftercooler inlet. This is because the temperature estimated at the intercooler inlet (160 °C) is greater than the temperature estimated at the aftercooler inlet (140 °C).

5 PRE-TEST MEASUREMENT UNCERTAINTY ESTIMATION

Measurement error is the difference between a measured value and its true value. Measurement uncertainty is different from the measurement error in that the uncertainty is the way to express and quantify the doubt or ambiguity in a measurement. There are two main types of errors in measurement uncertainty; systematic errors and random errors. Systematic errors are also known as bias errors and they remain constant during repeatability of measurements. These systematic errors can be reduced by calibration because there is more uncertainty when instruments are not calibrated. Random errors are also known as precision errors and they differ randomly during repeatability of measurement. These errors can be minimized through statistical principles by collecting larger data sets. (Bell, 1999; ASME PTC 19.1, 2006.)

According to ASME PTC 19.1-2005 (2006) (Test Uncertainty), uncertainty analysis can be done by determining the error sources which could be from five main sources;

- Uncertainty due to calibration: Calibration helps to reduce systematic errors to acceptable levels. The calibration uncertainty usually accompanies the instrument documentation.

- Uncertainty due to differences between the calibration laboratory and the installation on the field. An example may be differing environmental conditions from the calibration conditions and the instrumentation conditions etc.

- Uncertainty due to data acquisition: These arise from sensors, recording devices, etc. but the errors can be minimized by conducting an overall calibration of the measurement system if possible.

- Uncertainty due to data reduction: These usually result from curve fits, computational resolution, assumptions, constants, approximating relationships used in the calculation procedure, etc.

- Uncertainty due to methods: These result from methods used in the measurement process and they can greatly affect the overall results.

There are two methods of estimating standard uncertainties according to the ISO/IEC GUIDE 98-3:2008 (Uncertainty of measurement – Part 3: Guide to the expression of uncertainty in measurement; GUM:1995.) They are Type A evaluation and Type B evaluation. Type A evaluation can be done by statistical methods when there is data and a series of observations from which the standard deviations can be calculated. Type B evaluations are used when there are no data to estimate the uncertainty, thus uncertainty evaluation is done by using other sources such as calibration certificates, manufacturer specifications, uncertainties in reference handbooks, logical judgment, and general knowledge.

Type B evaluation should be mainly used for pre-test measurement uncertainty analysis unless previous measurement data are available. For this thesis, manufacturer's specifications were used in the measurement uncertainty estimation for Type B estimation. The pre-test uncertainty analysis was done to determine the expected measurement uncertainty from the performance test. This helped to detect what measurement alternative gives an uncertainty within which the results are viable and acceptable. It also helps to know from which factors and parameters uncertainty can be minimized through better instrumentation, calibration, and measurement methods.

5.1 Method of uncertainty estimation

In estimating measurement uncertainty, all individual uncertainties from each instrument need to be converted to the same unit by converting them into relative uncertainty before

they can be combined. It is not possible to combine uncertainties of temperature measurements in ℃ to uncertainties of pressure measurements in a different unit. In the estimation of uncertainty from instruments, the accuracy limits in ASME PTC 13-2018 (2019) and the accuracy of measurement instruments from manufacturer's specification were used.

5.1.1 Uncertainty of measuring temperature

When estimating uncertainties from instruments with "of reading" (o.r.) values, Equation (12) was used. Such instruments with o.r. values are temperature measurement instruments.

$$Relative\ uncertainty\ (\frac{u(T)}{T}) = \frac{uncertainty\ (u(T))}{measured\ quantity\ (T)}\,, \tag{12}$$

where the $\frac{u(T)}{T}$ is the relative uncertainty in temperature, the $u(T)$ is the uncertainty in temperature (instrument accuracy of the temperature sensor indicated by the manufacturer), and T is the temperature measured.

Many manufacturers specify the accuracy of temperature instruments to be ± 0.1℃ of reading. According to Texas Instruments and Tricor Coriolis Technology datasheets, the accuracy of a Pt100 temperature sensor and an RTD in a Coriolis meter respectively were both stated as ±0.1 ℃. In the example below, a Pt100 temperature sensor of ± 0.1 ℃ accuracy is used to measure a temperature of 20 ℃. Equation (12) is applied to determine the relative uncertainty for temperature. The result (0.5%) is thus the relative uncertainty when a temperature of 20 ℃ is measured.

$$\frac{u(T)}{T} = \frac{0.1℃}{20℃} = \pm 0.5\%\,.$$

The relative uncertainty changes for the temperature measurements inside the compressor unit because of different temperature measured inside the unit. However, when there are multiple measurements that leads to averaging of the results (for instance, when there are four temperature instruments at the outlet of the compressor), a combination of Equation (12) and Equation (13) is used to derive the uncertainty from the mean. Equation (13) is in accordance with ASME PTC 19.1-2005 (2016).

$$u_{\bar{x}}(T) = \frac{u(T)}{\sqrt{n}}\,, \tag{13}$$

where $u_{\bar{x}}$ is the uncertainty of the mean temperature, $u(T)$ is the uncertainty in temperature (accuracy indicated by the manufacturer), n is the number of measurements.

Therefore, in the measurement configuration where there are four temperature measuring instruments, Equation (12) and Equation (13) is used to determine the relative uncertainty as shown in the example below. In the example, the temperature measured is 30 ℃ and each temperature sensor have an accuracy of ±0.1 ℃.

$$u_{\bar{x}}(T) = \frac{0.1\ ℃}{\sqrt{4}} = 0.05\ ℃$$

$$\frac{u_{\bar{x}}(T)}{T} = \frac{0.05℃}{30\ ℃} = \pm 0.17\%$$

5.1.2 Uncertainty of measuring pressure

According to Vaisala datasheet (2018), the instrument accuracy at 20 ℃ for a digital barometer is ±0.1 hPa for a barometric pressure range of 500 to 1100 hPa. The relative uncertainty of ambient pressure can thus be calculated as shown below using Equation (12).

$$\frac{u(P_{amb.})}{P_{amb.}} = \frac{0.1\ hPa}{1000\ hPa} = \pm 0.01\%$$

where the relative uncertainty in the ambient pressure, $\frac{u(P_{amb.})}{P_{amb.}}$ is equal to $\pm 0.01\%$.

When measuring pressure inside the compressor unit and at the outlet of the compressor unit, the full scale accuracy given by the manufacturer is used as the relative uncertainty. For a 4…20 mA pressure transmitter from Gefran (2016), the full scale (f.s.) accuracy is 0.5%. This accuracy is the relative uncertainty of the pressure and it is used for all pressure measurements. Therefore, $\frac{u(P)}{P} = \pm 0.5\%$.

When measuring the outlet pressure of the compressor unit with four pressure transmitters, the relative uncertainty of the average measurement is calculated by dividing the full scale uncertainty by the square root of the number of measurements. In the example below, the f.s. accuracy from manufacturer (relative uncertainty) for one instrument is ±0.5%.

$$\frac{u_{\bar{x}}(P)}{P} = \frac{\frac{u(P)}{P}}{\sqrt{4}} = \frac{0.5\%}{\sqrt{4}} = \pm 0.25\%$$

5.1.3 Uncertainty of measuring flow, relative humidity, rotational speed and power

When computing the uncertainty of flow rate for Coriolis meters, the basic accuracy in percentage indicated by the manufacturer is used as the relative uncertainty because Coriolis meters directly measure mass flow. Tricor instruments indicates the basic accuracy of Coriolis meter for gas applications as ±0.5% of flow rate (this was used in the uncertainty calculations).

When computing the uncertainty of flow rate for cone meter and ultrasonic meter, the method of propagation of uncertainty was used to estimate the relative uncertainty in mass flow rate. This is because cone meter and USM are volume flow meters, therefore, the uncertainty in the temperature and pressure should be accounted for in the mass flow rate uncertainty. Equation (14) is used for computing the relative uncertainty in mass flow.

$$\frac{u(q_m)}{q_m} = \sqrt{\left(\frac{u(q_v)}{q_v}\right)^2 + \left(\frac{u(T)}{T}\right)^2 + \left(\frac{u(P)}{P}\right)^2}. \tag{14}$$

The uncertainty of V-Cone meters according to McCrometer (2017) is ±0.5% of flow rate and Transus instruments datasheet have the typical accuracy of USM as ±0.5%. These accuracies were used for computing the relative uncertainty in the mass flow rate. An example using Equation (14) is shown below for a compressor unit outlet temperature measured at 30 ℃ using four temperature instruments and four pressure instruments in a manifold.

$$\frac{u(q_m)}{q_m} = \sqrt{(0.5\%)^2 + (0.17\%)^2 + (0.25\%)^2} = \pm 0.58\%$$

The accuracy of hygrometers from PCE Instruments for a measurement range of 0 to 100% RH is ±2.0% RH at 25 ℃. This instrument accuracy is used as the relative uncertainty of the relative humidity. The relative uncertainty used for rotational speed is in accordance with ASME PTC 13-2018 (2019) which indicates that the instrument used in measuring the rotational speed should have an accuracy that is at least ±0.15%. ASME PTC 13-2018 (2019) also indicates that the minimum accuracy of the power analyzer should be ±0.2% of reading for the basic power.

5.1.4 Overall measurement uncertainty

The Table 5 summarizes and shows the relative uncertainties from the instruments used in the estimation of the relative uncertainty and calculation of the measurement uncertainty.

Table 5. The relative uncertainties using instrument accuracies as uncertainties at the operation values used for the calculations

Measurement location	Instrument accuracy	Estimated measured value	Relative uncertainty
Barometric pressure	0.1 hPa	1000 hPa	±0.01%
Ambient temperature	0.1 ℃	20 ℃	±0.5%
Relative humidity	2% RH	-	±2%
First stage outlet T	0.1 ℃	160 ℃	±0.06%
Second stage inlet T	0.1 ℃	30 ℃	±0.33%
Second stage outlet T	0.1 ℃	140 ℃	±0.07%
Aftercooler outlet T	0.1 ℃	30 ℃	±0.33%
Pressure measurements	±0.5% FS	-	±0.5%
Compressor unit outlet pressure measurement with four instruments	±0.5% FS	-	±0.25%
Compressor unit outlet temperature measurement with four instruments	0.1 ℃	30 ℃	±0.17%
Rotational speed	±0.15%	-	±0.15%
Power	±0.2%	-	±0.2%
Mass flowmeter (Coriolis)	±0.5%	-	±0.5%
Volume flowmeter (Cone meter)	±0.5%	-	±0.58%*
Volume flowmeter (USM meter)	±0.5%	-	±0.58%*

* - the relative uncertainty in mass flow rate

In volume flowmeters (cone meter and ultrasonic meter), the uncertainty in the mass flow when using volume flowmeters increases to 0.58% because uncertainties in temperature and pressure were accounted for. This is because the mass flow in volume flowmeters depend on the temperature and pressure instruments (there were four pressure and four temperature instruments at the outlet of the compressor unit).

In the uncertainty calculation process of the compressor performance, sources of uncertainty in every calculation step was identified and the relative uncertainties from Table 5 were combined. The process of identifying the sources of uncertainty and combining the uncertainties is shown in Figure 19 below.

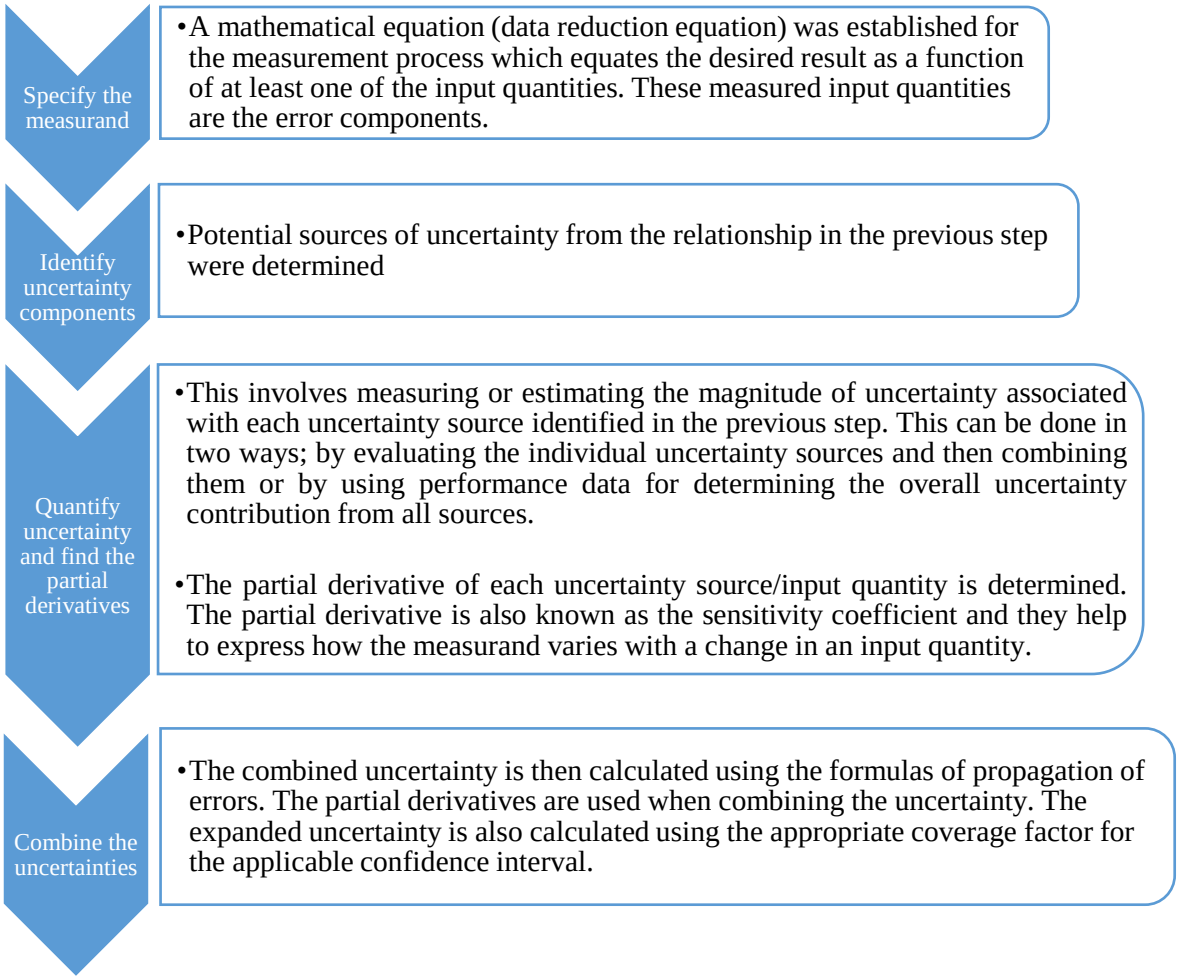

Figure 19. Steps for estimating the measurement uncertainty (Ellison and Williams, 2012; AGA Report No. 11, 2013).

The law of propagation of uncertainty was used to combine the individual uncertainties by using the root sum of squares as shown in Equation (15) and the expanded uncertainty is derived using Equation (16) (Bell 1999).

$$\frac{u(y)}{y} = \sqrt{\left[\left(\frac{\partial y}{\partial x_1}\right)^2 \cdot \left(\frac{u(x_1)}{x_1}\right)^2\right] + \left[\left(\frac{\partial y}{\partial x_2}\right)^2 \cdot \left(\frac{u(x_2)}{x_2}\right)^2\right] + \cdots + \left[\left(\frac{\partial y}{\partial x_n}\right)^2 \cdot \left(\frac{u(x_n)}{x_n}\right)^2\right]}, \quad (15)$$

where $\frac{u(y)}{y}$ is the relative uncertainty in the measurand y, $x_1 \ldots x_n$ are input variables that contribute to uncertainty, $\frac{\partial y}{\partial x_1} \ldots \frac{\partial y}{\partial x_n}$ are the partial derivatives (also known as sensitivity coefficients) of the input variables, $\left(\frac{u(x_1)}{x_1}\right)^2 \ldots \left(\frac{u(x_n)}{x_n}\right)^2$ are the relative uncertainties of the uncertainty contributory sources.

The uncertainties were combined at every step of the efficiency calculation process. The expanded uncertainty used for a normal distribution is then calculated using Equation (16) with a coverage factor of 2 for a 95% confidence interval. (Bell 1999).

$$U = k\frac{u(y)}{y} \quad (16)$$

where U is the relative expanded uncertainty, k as the coverage factor is equal to 2, $\frac{u(y)}{y}$is the relative uncertainty of y which was calculated from Equation (15).

For example, when determining the combined uncertainty in the pressure of vapor for the first stage compressor, the mathematical equation for pressure of vapor in Equation (17) helps to calculate the combined uncertainty. The uncertainty of RH comes from the hygrometer and the uncertainty of p_{sv} comes from the temperature instrument for measuring ambient temperature

$$p_{vp} = RH \cdot p_{\mathrm{sv}} \quad (17)$$

$$\frac{u(p_{vp})}{p_{vp}} = \sqrt{\left[\left(\frac{\partial p_{vp}}{\partial RH}\right)^2 \cdot \left(\frac{u(RH)}{RH}\right)^2\right] + \left[\left(\frac{\partial p_{vp}}{\partial p_{sv}}\right)^2 \cdot \left(\frac{u(p_{sv})}{p_{sv}}\right)^2\right]}$$

$$= \sqrt{[1^2 \cdot (2\%)^2] + [1^2 \cdot (0.58\%)^2]} = \pm 2.08\%,$$

$$U_{p_{vp},95} = 2 \cdot \frac{u(p_{vp})}{p_{vp}} = 2 \cdot 2.08\% = \pm 4.16\%$$

This method of determining the expanded uncertainty was used throughout the determination of the measurement uncertainty.

5.2 Results of measurement uncertainty

The uncertainty in the pressure ratio, efficiency, and the mass flow rate was calculated for all three measurement scenarios while also comparing the four measurement setups based on different flowmeter use. The measurement uncertainty results in this chapter are for single measurements and they were done using the calculated and manufacturer's specifications in Table 5. An example calculation of the uncertainty calculation is also included in the Appendix.

5.2.1 Uncertainty in measurement scenario 1 and measurement scenario 2

The results of uncertainty are calculated using the estimated inlet and outlet conditions shown below;

- Ambient temperature – 20 ℃
- Ambient pressure – 100 kPa
- Relative Humidity – 90%
- Pressure loss in the compressor unit inlet filter – 3 kPa
- Compressor outlet temperature – 30 ℃
- Compressor unit outlet pressure – 750 kPa
- Pressure at reference conditions – 101.325 kPa
- Temperature at reference conditions – 20 ℃
- Relative humidity at reference conditions – 0%

5.2.1.1 Expanded uncertainty in pressure ratio

The uncertainty in pressure ratio is calculated from the uncertainties in the inlet and outlet pressure measurement instruments. Equation (18) is the pressure ratio formula, Equation

(19) is used to calculate the uncertainty in pressure ratio, and Equation (20) is used to determine the expanded uncertainty in the pressure ratio at 95% confidence interval.

$$\pi = \sqrt{\frac{p_2}{p_1}} \tag{18}$$

$$\frac{u(\pi)}{\pi} = \sqrt{\left[\left(\frac{\partial \pi}{\partial p_2}\right)^2 \cdot \left(\frac{u(p_2)}{p_2}\right)^2\right] + \left[\left(\frac{\partial \pi}{\partial p_1}\right)^2 \cdot \left(\frac{u(p_1)}{\mathrm{p_1}}\right)^2\right]} \tag{19}$$

$$U_{\pi,95} = 2 \cdot \frac{u(\pi)}{\pi} \tag{20}$$

When Equations (19) and (20) are combined, the expanded uncertainty in the pressure ratio for measurement scenarios 1 and 2 are calculated below.

$$U_{\pi,95} = 2 \cdot \sqrt{\left[\left(\frac{1}{2}\right)^2 \cdot (0.25\%)^2\right] + \left[\left(\frac{1}{2}\right)^2 \cdot (0.02\%)^2\right]} = 0.25\%$$

The above result shows that the expanded uncertainty in pressure ratio is 0.25%. In the calculation process, $\frac{\partial \pi}{\partial p_2}$ and $\frac{\partial \pi}{\partial p_1}$ are the partial derivatives. The relative uncertainty in compressor unit outlet pressure $\frac{u(p_2)}{p_2}$ is obtained from uncertainty of the mean of four pressure instruments in a manifold. The relative uncertainty in compressor unit inlet pressure $\frac{u(p_1)}{p_1}$ is obtained from the uncertainty in the ambient pressure instrument and the instrument for determining the pressure difference in the air filter before the first stage compressor.

5.2.1.2 Expanded uncertainty in mass flow at the compressor unit inlet

The uncertainty in mass flow at the inlet of the compressor unit is calculated from the uncertainty in the mass flow measured at the compressor unit outlet, the humidity ratios at the inlet and the outlet of the compressor unit. Equation (21) is the mass flow at the inlet of the compressor unit, Equation (22) is used to calculate the uncertainty in mass flow at the inlet of the compressor unit, and Equation (23) is used to determine the expanded uncertainty in the mass flow at the inlet of the compressor unit at 95% confidence interval.

$$q_{\mathrm{m},1} = q_{\mathrm{m},2} \cdot \left(\frac{1+HR_1}{1+HR_2}\right) \tag{21}$$

$$\frac{u(q_{m,1})}{q_{m,1}} = \sqrt{\left[\left(\frac{\partial q_{m,1}}{\partial q_{\mathrm{m},2}}\right)^2 \cdot \left(\frac{u(q_{\mathrm{m},2})}{q_{\mathrm{m},2}}\right)^2\right] + \left[\left(\frac{\partial q_{m,1}}{\partial HR_1}\right)^2 \cdot \left(\frac{u(HR_1)}{HR_1}\right)^2\right] + \left[\left(\frac{\partial q_{m,1}}{\partial HR_2}\right)^2 \cdot \left(\frac{u(HR_2)}{HR_2}\right)^2\right]} \quad (22)$$

$$U_{\mathrm{q_{m,1}}} = 2 \cdot \frac{u(q_{\mathrm{m},1})}{q_{\mathrm{m},1}} \quad (23)$$

When Equation (22) and (23) are combined, the expanded uncertainty is measurement scenarios 1 and 2 are calculated below for different flowmeter configurations as shown below.

For conemeter,

$$U_{q_{m,1,95}} = 2 \cdot \sqrt{[1^2 \cdot (0.58\%)^2] + \left[\left(\frac{1}{\frac{1}{HR_1}+1}\right)^2 \cdot (2.08\%)^2\right] + \left[\left(\frac{1}{\frac{1}{HR_2}+1}\right)^2 \cdot (0.32\%)^2\right]} = 1.17\%$$

For ultrasonic meter,

$$U_{\mathrm{q_{m,1,95}}} = 2 \cdot \sqrt{[1^2 \cdot (0.58\%)^2] + \left[\left(\frac{1}{\frac{1}{HR_1}+1}\right)^2 \cdot (2.08\%)^2\right] + \left[\left(\frac{1}{\frac{1}{HR_2}+1}\right)^2 \cdot (0.32\%)^2\right]} = 1.17\%$$

For Coriolis meter with four temperature measuring instruments,

$$U_{q_{m,1},95} = 2 \cdot \sqrt{\begin{matrix}[1^2 \cdot (0.5\%)^2] + \left[\left(\frac{1}{\frac{1}{HR_1}+1}\right)^2 \cdot (2.08\%)^2\right] \\ + \left[\left(\frac{1}{\frac{1}{HR_2}+1}\right)^2 \cdot (0.32\%)^2\right]\end{matrix}} = 1\%$$

For Coriolis meter without four temperature measuring instruments,

$$U_{q_{m,1},95} = 2 \cdot \sqrt{\begin{matrix}[1^2 \cdot (0.5\%)^2] + \left[\left(\frac{1}{\frac{1}{HR_1}+1}\right)^2 \cdot (2.08\%)^2\right] \\ + \left[\left(\frac{1}{\frac{1}{HR_2}+1}\right)^2 \cdot (0.46\%)^2\right]\end{matrix}} = 1\%$$

HR_1 is calculated from measurements at the inlet of the compressor unit (measurements of ambient temperature, ambient pressure, and relative humidity). HR_2 is calculated from the pressure and temperature measurement at the outlet of the compressor unit.

The result shows that the expanded uncertainty in mass flow at the compressor unit inlet is the same when the Coriolis meter is used with or without the four temperature instruments. This means when using a Coriolis meter, the use of four temperature instruments for deriving the average temperature at the outlet does not affect the expanded uncertainty even though it has an effect on the uncertainty of the HR at the compressor unit outlet. The expanded uncertainty is higher for cone meter and ultrasonic meter (both 1.17%) because the basic accuracy of both volume flowmeters is 0.5% which increases to 0.58% in mass flow when the temperature and pressure are accounted for.

5.2.1.3 Expanded uncertainty in isentropic efficiency

The uncertainty in the isentropic efficiency for measurement scenarios 1 and 2 arises from uncertainty contributory sources which are isentropic exponent (κ), inlet mass flow ($q_{m,1}$),

specific gas constant of the mixture (R), inlet temperature (T_1), pressure ratio (π), and actual input power ($\dot{W}_{\mathrm{act}}$). Equation (24) is the isentropic efficiency,

$$\eta_{\mathrm{is}} = \frac{Ideal\ input\ power}{Actual\ input\ power} = \frac{\dot{W}_{\mathrm{is}}}{\dot{W}_{\mathrm{act}}} = \frac{\frac{\kappa}{\kappa-1} q_{\mathrm{m},1} R T_1 (\pi^{\frac{\kappa-1}{\kappa}} - 1)}{\dot{W}_{\mathrm{act}}}. \tag{24}$$

The partial derivative of the ideal input power ($\dot{W}_{\mathrm{is}}$) is used to determine the relative uncertainty in the ideal input power as shown in Equation (25).

$$\frac{u(\dot{W}_{\mathrm{is}})}{\dot{W}_{\mathrm{is}}} = \sqrt{\begin{aligned}&\left[\left(-\frac{1}{\kappa-1} + \frac{\pi^{\frac{\kappa-1}{\kappa}} \ln(\pi)}{\kappa}\right)^2 \cdot \left(\frac{u(\kappa)}{\kappa}\right)^2\right] + \left[1^2 \cdot \left(\frac{u(q_{\mathrm{m},1})}{q_{\mathrm{m},1}}\right)^2\right] + \left[1^2 \cdot \left(\frac{u(R)}{R}\right)^2\right] \\ &+ \left[1^2 \cdot \left(\frac{u(T_1)}{T_1}\right)^2\right] + \left[\left(\frac{(\kappa-1)\left(\pi^{\frac{-1}{\kappa}}\right)}{\frac{\kappa}{\pi}\left(\frac{\pi^{\frac{\kappa-1}{\kappa}}-1}{\pi}\right)}\right)^2 \cdot \left(\frac{u(\pi)}{\pi}\right)^2\right]\end{aligned}} \tag{25}$$

The result from Equation (25) is then substituted into Equation (26) to determine the uncertainty in the isentropic efficiency.

$$\frac{u(\eta_{\mathrm{is}})}{\eta_{\mathrm{is}}} = \sqrt{\left[\left(\frac{\partial \eta_{\mathrm{is}}}{\partial \dot{W}_{\mathrm{is}}}\right)^2 \cdot \left(\frac{u(\dot{W}_{\mathrm{is}})}{\dot{W}_{\mathrm{is}}}\right)^2\right] + \left[\left(\frac{\partial \eta_{\mathrm{is}}}{\partial \dot{W}_{\mathrm{act}}}\right)^2 \cdot \left(\frac{u(\dot{W}_{\mathrm{act}})}{\dot{W}_{\mathrm{act}}}\right)^2\right]} \tag{26}$$

The expanded uncertainty in the isentropic efficiency is then determined using Equation (27) below.

$$U_{\eta_{\mathrm{is}},95} = 2 \cdot \frac{u(\eta_{\mathrm{is}})}{\eta_{\mathrm{is}}} \tag{27}$$

The results of the expanded uncertainties in pressure ratio, mass flow, and isentropic efficiency for measurement scenarios 1 and 2 are shown in Table 6 below. Both scenarios give the same result since the uncertainty sources come from the same instruments even though the second stage outlet temperature is used in the measurement scenario 2. The results of the expanded uncertainties are summarized as shown in Table 6.

Table 6. The measurement uncertainty in measurement scenarios 1 and 2

Expanded uncertainty	Measurement scenario 1	Measurement scenario 2
$U_{\pi,95}$	±0.25%	±0.25%
$U_{q_{m,1},95}$(Cone meter)	±1.17%	±1.17%
$U_{q_{m,1},95}$(USM)	±1.17%	±1.17%
$U_{q_{m,1},95}$(Coriolis meter)	±1%	±1%
$U_{q_{m,1},95}$(Coriolis meter with four temperature instruments)	±1%	±1%
$U_{\eta_{is},95}$ (Cone meter)	±3.66%	±3.66%
$U_{\eta_{is},95}$ (USM)	±3.66%	±3.66%
$U_{\eta_{is},95}$ (Coriolis meter)	±3.61%	±3.61%
$U_{\eta_{is},95}$ (Coriolis meter with four temperature instruments)	±3.61%	±3.61%

Based on the results in Table 6, it does not make any difference in terms of accuracy if an ultrasonic meter and a cone meter are used. This is because the basic accuracy used for both volume flowmeters were 0.5%. However, ultrasonic flowmeters can still be flow calibrated to 0.1% -0.2% of reading for the entire calibration range based on several manufacturers' specifications. This would make them more accurate than cone meters but the USM still requires long upstream and downstream lengths compared to cone meter.

The results also show that Coriolis meters have the least uncertainty in the mass flow of the compressor unit (±1%) and the isentropic efficiency (±3.61%). However, there is no effect on the mass flow or efficiency uncertainty if four temperature instruments are added to the Coriolis meter configuration. Nonetheless, it is important to note that there are some weak-nesses to calculating the efficiency of the compressor using measurement scenarios 1 and 2

because processes inside the compressor unit are not known or are neglected in the uncertainty calculation. Important factors that are neglected include the intercooling process which is affected by the temperature of the liquid used for cooling. Intercooling is an essential part of two-stage dry screw compressors.

5.2.1.4 Expanded uncertainty in the calculations back to reference conditions

The uncertainty in the mass flow when calculated back to reference conditions was calculated using Equation (30).

For mass flow at reference conditions,

$$q_{\mathrm{m,ref}} = q_{\mathrm{m}} \cdot \frac{p_{1,\mathrm{ref}}}{p_1} \sqrt{\frac{T_1 R}{T_{1,\mathrm{ref}} R_{\mathrm{ref}}}}, \tag{28}$$

$$\frac{u(q_{\mathrm{m,ref}})}{q_{\mathrm{m,ref}}} = \sqrt{\begin{matrix}\left[\left(\frac{\partial q_{\mathrm{m,ref}}}{\partial q_{\mathrm{m}}}\right)^2 \cdot \left(\frac{u(q_{\mathrm{m}})}{q_{\mathrm{m}}}\right)^2\right] + \left[\left(\frac{\partial q_{\mathrm{m,ref}}}{\partial \mathrm{p}_1}\right)^2 \cdot \left(\frac{u(p_1)}{p_1}\right)^2\right] \\ + \left[\left(\frac{\partial q_{\mathrm{m,ref}}}{\partial T_1}\right)^2 \cdot \left(\frac{u(T_1)}{T_1}\right)^2\right] + \left[\left(\frac{\partial q_{\mathrm{m,ref}}}{\partial \mathrm{R}}\right)^2 \cdot \left(\frac{u(R)}{R}\right)^2\right]\end{matrix}} \tag{29}$$

The partial derivatives are then substituted into Equation (29) to determine the expanded uncertainty at 95% interval.

$$U_{\mathrm{q_{m,ref},95}} = 2 \cdot \sqrt{\begin{matrix}\left[1^2 \cdot \left(\frac{u(q_{\mathrm{m}})}{q_{\mathrm{m}}}\right)^2\right] + \left[-1^2 \cdot \left(\frac{u(p_1)}{p_1}\right)^2\right] \\ + \left[\left(\frac{1}{2}\right)^2 \cdot \left(\frac{u(T_1)}{T_1}\right)^2\right] + \left[\left(\frac{1}{2}\right)^2 \cdot \left(\frac{u(R)}{R}\right)^2\right]\end{matrix}} \tag{30}$$

The expanded uncertainties of mass flow at reference conditions are below.

$U_{\mathrm{q_{m,ref},95}} = \pm 1.76\%$ for cone meter

$U_{\mathrm{q_{m,ref},95}} = \pm 1.76\%$ for ultrasonic meter

$U_{\mathrm{q_{m,ref},95}} = \pm 1.65\%$ for Coriolis meter

The uncertainty of $\pm 1.65\%$ in the mass flow at reference conditions for Coriolis meter is better than in cone meter and ultrasonic meter because the uncertainty in mass flow of Coriolis meter is better than the uncertainties in the mass flow of cone meter and ultrasonic meter.

The uncertainty in the rotational speed and power when calculated back to reference conditions was calculated using Equations (33) and (36) respectively. The flowmeter option does not affect the uncertainty estimate of speed and power at reference conditions but it affects the uncertainty in the mass flow at reference conditions. This is because the uncertainty sources for speed at reference condition is dependent on the measured speed, specific gas constant, and temperature at inlet conditions. Also, the uncertainty of power at reference conditions is dependent on the uncertainties of the measured speed and power.

For the rotational speed at reference conditions,

$$N_{\mathrm{ref}} = N\sqrt{\frac{T_{1,\mathrm{ref}}\,R_{\mathrm{ref}}}{T_1 R}}\,, \tag{31}$$

$$\frac{u(N_{\mathrm{ref}})}{N_{\mathrm{ref}}} = \sqrt{\left[\left(\frac{\partial N_{ref}}{\partial N}\right)^2 \cdot \left(\frac{u(N)}{N}\right)^2\right] + \left[\left(\frac{\partial N_{ref}}{\partial T_1}\right)^2 \cdot \left(\frac{u(T_1)}{T_1}\right)^2\right] + \left[\left(\frac{\partial N_{ref}}{\partial R}\right)^2 \cdot \left(\frac{u(R)}{R}\right)^2\right]} \tag{32}$$

The partial derivatives are then substituted into Equation (32) to determine the expanded uncertainty at 95% confidence interval for the speed at reference conditions.

$$U_{N_{\mathrm{ref}},95} = 2 \cdot \sqrt{\left[1^2 \cdot \left(\frac{u(N)}{N}\right)^2\right] + \left[\left(\frac{1}{2}\right)^2 \cdot \left(\frac{u(T_1)}{T_1}\right)^2\right] + \left[\left(\frac{1}{2}\right)^2 \cdot \left(\frac{u(R)}{R}\right)^2\right]} \tag{33}$$

The results of the expanded uncertainty of speed at reference condition at 95% confidence interval is:

$$U_{\mathrm{N,ref},95} = \pm 1.34\%$$

For power at reference conditions,

$$P_{\mathrm{ref}} = \left(\frac{N_{\mathrm{ref}}}{N}\right)^2 \cdot P\,, \tag{34}$$

$$\frac{u(P_{\mathrm{ref}})}{P_{\mathrm{ref}}} = \sqrt{\left[\left(\frac{\partial P_{\mathrm{ref}}}{\partial N_{\mathrm{ref}}}\right)^2 \cdot \left(\frac{u(N_{\mathrm{ref}})}{N_{\mathrm{ref}}}\right)^2\right] + \left[\left(\frac{\partial P_{\mathrm{ref}}}{\partial N}\right)^2 \cdot \left(\frac{u(N)}{N}\right)^2\right] + \left[\left(\frac{\partial P_{\mathrm{ref}}}{\partial P}\right)^2 \cdot \left(\frac{u(P)}{P}\right)^2\right]} \quad (35)$$

The partial derivative of P_{ref} are then substituted into Equation (35) to give the expanded uncertainty as shown below.

$$U_{\mathrm{P_{ref,95}}} = 2 \cdot \sqrt{\left[2^2 \cdot \left(\frac{u(N_{\mathrm{ref}})}{N_{\mathrm{ref}}}\right)^2\right] + \left[-2^2 \cdot \left(\frac{u(N)}{N}\right)^2\right] + \left[1^2 \cdot \left(\frac{u(P)}{P}\right)^2\right]} \quad (36)$$

The results of the expanded uncertainty in power at reference condition at 95% confidence interval is:

$$U_{\mathrm{P,ref,95}} = \pm 2.78\%$$

5.2.2 Uncertainty in measurement scenario 3

The expanded uncertainty in the pressure ratio, mass flow rate, and efficiency was calculated for the measurement scenario 3 with detailed measurement locations inside the compressor unit. Comparisons were also made in the efficiency measurement uncertainty when different flowmeter measurement setups are used. The uncertainty calculation process followed a similar process as in measurement scenarios 1 and 2. However, the pressure ratio was calculated using Equation (37), thus the uncertainty in the pressure ratio was calculated separately for the first stage and the second stage using Equation (38) because the pressure at the inlet and outlet of both stages are measured. Therefore, there was no assumption that the pressure ratio is equally divided between both stages.

$$\pi = \frac{p_2}{p_1} \quad (37)$$

$$\frac{u(\pi)}{\pi} = \sqrt{\left[1^2 \cdot \left(\frac{u(p_2)}{p_2}\right)^2\right] + \left[-1^2 \cdot \left(\frac{u(p_1)}{p_1}\right)^2\right]} \quad (38)$$

The mass flow at the inlet of the first stage and inlet of the second stage was calculated similarly to the process of calculations in measurement scenarios 1 and 2 using Equation (39) below.

$$q_{\mathrm{m,1}} = q_{\mathrm{m,2}} \cdot \left(\frac{1+HR_1}{1+HR_2}\right) \quad (39)$$

where $q_{\mathrm{m},1}$ is the mass flow at the inlet of the stage, $q_{\mathrm{m},2}$ is the mass flow at the outlet of the stage, HR_1 is the humidity ratio at the inlet of the stage, HR_2 is the humidity ratio at the outlet of the stage. This calculation was done for the first stage and the second stage.

The uncertainty in the mass flow was then calculated using Equation (40)

$$\frac{u(q_{m,1})}{q_{m,1}} = \sqrt{\left[1^2 \cdot \left(\frac{u(q_{\mathrm{m},2})}{q_{\mathrm{m},2}}\right)^2\right] + \left[\left(\frac{1}{\frac{1}{HR_1}+1}\right)^2 \cdot \left(\frac{u(HR_1)}{HR_1}\right)^2\right] + \left[\left(\frac{1}{\frac{1}{HR_2}+1}\right)^2 \cdot \left(\frac{u(HR_2)}{HR_2}\right)^2\right]} \tag{40}$$

The isentropic efficiency and the uncertainty in isentropic efficiency were calculated using Equations (41) and (42) respectively.

$$\eta_{\mathrm{is}} = \frac{\dot{W}_{\mathrm{is,first}} + \dot{W}_{\mathrm{is,second}}}{\dot{W}_{\mathrm{act}}} \tag{41}$$

$$\frac{u(\eta_{is})}{\eta_{is}} = \sqrt{\left[\left(\frac{1}{1+\frac{\dot{W}_{\mathrm{is,second}}}{\dot{W}_{\mathrm{is,first}}}}\right)^2 \cdot \left(\frac{u\left(\dot{W}_{\mathrm{is,first}}\right)}{\dot{W}_{\mathrm{is,first}}}\right)^2\right] + \left[\left(\frac{1}{\frac{\dot{W}_{\mathrm{is,first}}}{\dot{W}_{\mathrm{is,second}}}+1}\right)^2 \cdot \left(\frac{u\left(\dot{W}_{\mathrm{is,second}}\right)}{\dot{W}_{\mathrm{is,second}}}\right)^2\right] + \left[-1^2 \cdot \left(\frac{u\left(\dot{W}_{\mathrm{act}}\right)}{\dot{W}_{\mathrm{act}}}\right)^2\right]} \tag{42}$$

The uncertainty in pressure ratio at 95% confidence interval was calculated for each stage and the results are shown below.

$$U_{\pi_{\mathrm{first}},95} = \pm 1\%$$

$$U_{\pi_{second},95} = \pm 1.41\%$$

The pressure ratio uncertainty in the first stage is lower than the pressure ratio uncertainty in the second stage because the basic accuracy of the ambient pressure instrument (barometer)

is ±0.01% compared to the accuracy of other pressure measurement instruments (Pressure transmitter Pt100) which is ±0.5%.
The results of the uncertainty in mass flow and efficiency are presented in Table 7.

Table 7. Results of uncertainty in the efficiency and mass flow

Flowmeter options	$U_{\mathrm{q_m},95}$	$U_{\eta_{\mathrm{is}},95}$
Cone meter	±1.17%	±3.37%
Ultrasonic meter	±1.17%	±3.37%
Coriolis (without four temperature instruments)	±1%	±3.35%
Coriolis (with four temperature instruments)	±1%	±3.35%

The results from Table 7 shows that there is no difference in the uncertainty if the Coriolis meter configuration is with or without four temperature measurement instruments. The results show that measurement uncertainty in the mass flow and efficiency is lowest when a Coriolis meter is used. The isentropic efficiency uncertainty for all four flowmeter measurement options does not differ much from each other (0.02%) whereas there is a difference of ±0.17% in the mass flow uncertainty.

The uncertainties in the calculations back to reference conditions are based on the compressor unit inlet conditions. The uncertainty in the mass flow, speed, and power back to reference were calculated in accordance with the calculation process in measurement scenarios 1 and 2. The results are below.

$U_{\mathrm{q_{m,ref}},95} = \pm 1.76\%$ for cone meter

$U_{\mathrm{q_{m,ref}},95} = \pm 1.76\%$ for ultrasonic meter

$U_{\mathrm{q_{m,ref}},95} = \pm 1.65\%$ for Coriolis meter

$U_{\mathrm{N,ref},95} = \pm 1.34\%$

$U_{\mathrm{P,ref},95} = \pm 2.78\%$

From the results above, the uncertainty in the calculation back to reference conditions are the same in measurement scenario 3 compared to measurement scenario 1 and 2.

5.2.3 Comparison of uncertainty when ambient temperature is varied

To see how a change in ambient temperature affects the uncertainty in the efficiency, the ambient temperature was varied across five temperatures (10 ℃, 20 ℃, 25 ℃, 30 ℃ and 40 ℃) while other conditions are kept constant. In Figure 20, the effect of varying the ambient temperature in the case of using the Coriolis meter with four outlet temperature instruments was examined.

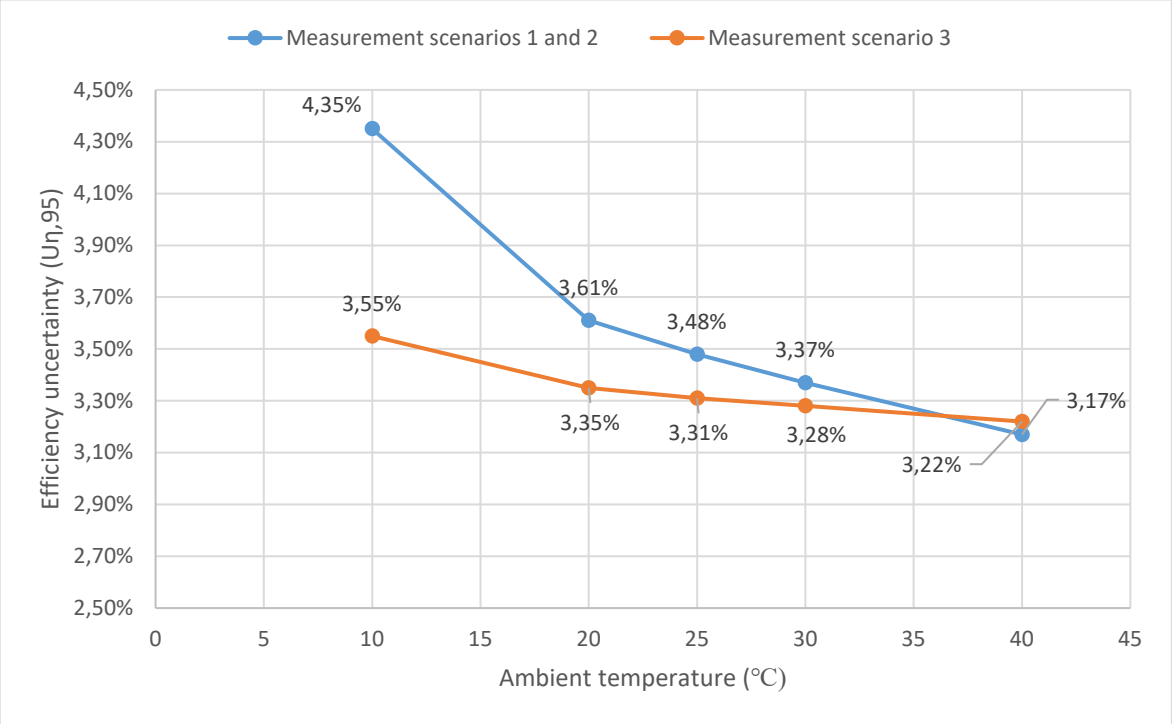

Figure 20. Effect of ambient temperature change on the efficiency uncertainty

Figure 20 shows that the uncertainty decreases when ambient temperature rises for all scenarios. It shows that the uncertainty decreases more steeply in measurement scenarios 1 and 2 where measurements were taken over the compressor unit without internal compressor unit measurements. The results show how the uncertainty increases more steeply when ambient temperature falls from 20℃ to 10℃ especially in measurement scenarios 1 and 2. The measurement uncertainty curve is more flattened in measurement scenario 3 where there is a de-

tailed measurement in the compressor unit. The results also show that there is lower uncertainty in measurement scenario 3. This is because the magnitude of the unknowns has been decreased in measurement scenario 3 as a result of making more measurements. However, there is more uncertainty in measurement scenarios 1 and 2 in Figure 20 due to the assumptions made, which thus lead to more uncertainty in results.

6 CONCLUSIONS AND DISCUSSION

The theoretical research and study in Chapter 2 conveyed a good understanding of how a two-stage dry screw compressor with a cooling system works, and the measurements and instruments needed when conducting a performance test. It showed that cooling is an important part of the whole compression system that needs to be acknowledged. As ambient conditions and flow measurement are also important, the operating principles of flow measurement options suitable for this application were elaborated. The theoretical research also reveals the importance of dry screw compressors in industrial applications.

Four measurement designs based on three different flowmeters were reviewed. The outcomes show that ultrasonic meter piping design is not feasible to mount in many industries due to the long inlet and outlet meter runs. This length requirement is the main weakness of ultrasonic meter even though it has a good accuracy level. Cone meter configurations have lower accuracy but more space requirement compared to Coriolis meter. Hence, the recommendation of Coriolis meter as a compact design with better accuracy compared to the other options. The measurement of the outlet temperature using four instruments helps with averaging of the temperature reading, and it acts as a temperature reference for the Coriolis meter. Although the four temperature measurement instruments in a Coriolis meter configuration does not affect the measurement uncertainty, it is still recommended by the standards to have four temperature measurement instruments. Overall, it is most feasible to mount the Coriolis meter piping setup in industries when conducting measurements due to its compactness.

The performance of the compressor was evaluated using isentropic efficiency. Steps were considered to determine which measurements will be enough to calculate the efficiency. The first step was measurement scenario 1 where there was no measurement inside the compressor unit. It was possible to calculate the mass flow at the inlet of the compressor unit in scenario 1. The main disadvantage in this scenario is that several assumptions related to

pressure ratio and actual input power were made. This raises the question of whether the compressor performance results are still accurate enough with the assumptions made. The next step taken was to solve the aftercooler effect by measuring the air temperature before the aftercooler, therefore measurement scenario 2 was devised. The main drawback of measurement scenario 2 was that intercooling effect was not accounted for and the efficiency calculation considers the compressor unit as a single-stage compressor. Assumptions in pressure ratio and actual work input were still made in measurement scenario 2.

Measurement scenario 3 with several measurements inside the compressor unit was then devised in order to reduce the magnitude of unknowns and assumptions in the efficiency calculations. Measurement scenario 3 is recommended because it accounts for intercooling and solves for the aftercooling effect. It also acknowledges and gives details that mass flow into the first stage is different from the mass flow into the second stage due to the removal of condensate water. Measurement scenario 1 does not give details on the division of condensate mass flows but still calculates the mass flow of the total condensate. Therefore, measurement scenario 3 is recommended because more information is given on the compression process. A Microsoft excel calculation tool that followed the steps of calculation in the measurement scenarios was made. The tool allows varying of several measurement variables to assess the isentropic efficiency results.

Type B evaluation was used for estimating the measurement uncertainty using manufacturers' specifications. There is reduced uncertainty in measurement scenario 3 compared to measurement scenarios 1 and 2 because of the more detailed measurement in scenario 3. There are no pressure ratio and actual input power assumptions in measurement scenario 3. The results also showed that the efficiency uncertainty is least when a Coriolis meter is used. However, the uncertainty in the Coriolis meter configuration when it includes four temperature instruments does not differ from when the four temperature instruments are not used. Nonetheless, the standards reviewed recommends having four temperature measurement instruments at the outlet of the compressor unit. The results also show that the increase in ambient temperature reduces uncertainty. There is more steepness in the efficiency uncertainty in measurement scenarios 1 and 2 compared to measurement scenario 3. In all measurement scenarios, the presence of a dryer (dry air) or absence of a dryer (wet air) does not

have any effect on the uncertainty calculations. Nonetheless, the method, calculation process, and model for estimating the compressor performance in this thesis still needs to be validated. This validation can be done either by conducting tests in the laboratory or in an industrial environment, thus actual measured values are used.

For future research, for the possibility to vary inlet cooling liquid temperature, the flow division of the liquid for cooling needs to be known. Further research could be done to determine the magnitude of liquid cooling temperature directly on the efficiency to see how the temperature of liquid affects the efficiency and the second stage inlet temperature. Data on the oil (if at all it has a significant effect) may be needed to make a better assessment oF the effects of oil on the compressor efficiency. The type of oil, viscosity, flow rate, and temperatures of oil too may help to assess oil effects on efficiency.

REFERENCES

ABB Automation Products GmbH (2011). *Industrial Flow Measurement*. Basics and Practice.

American Gas Association (2013). *AGA Report No. 11. Measurement of Natural Gas by Coriolis Meter*. second Edition. Washington, DC 20001.

American Gas Association (2017). *AGA Report No. 9. Measurement of Gas by Multipath Ultrasonic Meters*. 3rd Edition. Washington, DC 20001.

Apple, C., Anklin, M., and Drahm, W. (2003). Section 2.11: Mass Flow meters, Coriolis. In: B. Lipták, ed., *Instrument Engineers' Handbook: Process Measurement and Analysis*, 4th ed. Boca Raton, FL: CRC Press

Atlas Copco (2018). *Oil-free air rotary screw compressors – ZR 90-160 VSD+ (FF*). Wilrijk: Atlas Copco Airpower NV.

Atlas Copco (2019). *Compressed Air Manual*. 9th ed. Wilrijk: Atlas Copco Airpower NV.

Bell, S. (1999). Measurement Good Practice Guide No. 11. *A Beginner's Guide to Uncertainty of Measurement*, (2).

Brasz, J. (2006). Comparison of Part-Load Efficiency Characteristics of Screw and Centrifugal Compressors. In: *International Compressor Engineering Conference*. [online] Available at: http://docs.lib.purdue.edu/icec/1827 [Accessed 14 Jan. 2020].

Brown, R. (2011). *Compressors-Selection and Sizing*. 3rd ed. Burlington: Elsevier Science. ISBN 0-7506-7545-4

Calame, S. (2013). *Fundamentals Of Coriolis Meters*. AGA Report 11. [online] Colorado. Available at: <https://asgmt.com/wp-content/uploads/pdf-docs/2013/1/002.pdf> [Accessed 16 April 2020].

Dong, F., Tan, C., Li, W. and Zhang, F. (2009). Flow rate measurement of oil-water two-phase flow based on V-cone flow meter. *Journal of Physics: Conference Series*, [online] 147, p.012059. Available at: https://www.researchgate.net/publication/243673643_Flow_rate_measurement_of_oil-water_two-phase_flow_based_on_V-cone_flow_meter [Accessed 27 Jan. 2020].

Emerson Electric (2019). *Daniel SeniorSonic 3414 Four-Path Gas Ultrasonic Flow Meter*.

Finnish Ministry of Economic Affairs and Employment (2019). *Finland's Integrated Energy And Climate Plan*. Helsinki: Ministry of Economic Affairs and Employment. Available at http://urn.fi/URN:ISBN:978-952-327-478-5

Fofanov, A. (2015). *Power efficiency estimation and simulation of different control methods for the rotary screw compressor*. M.Sc. LUT University. Available at https://lutpub.lut.fi/bitstream/handle/10024/104718/Theis_Fofanov.pdf?sequence=3&isAllowed=y .

Gefran (2016). *NaK Filled MELT pressure transmitters. Series KE 4…20 mA output*

International organization for Standardization (2003). *ISO 5167-1, Measurement of fluid flow by means of pressure differential devices – Part 1: Orifice plates, nozzles and Venturi tubes inserted in circular cross-section conduits running full*, ue de Stassart, 36 B-1050 Brussels

International organization for Standardization (2008). *ISO/IEC GUIDE 98-3, Uncertainty of measurement – Part 3: Guide to the expression of uncertainty of uncertainty in measurement*. Geneva, Switzerland

International organization for Standardization (2009). *ISO 1217, Displacement compressors – Acceptance tests*. Geneva, Switzerland

International organization for Standardization (2016). *ISO 5167-5, Measurement of fluid flow by means of pressure differential devices inserted in circular cross section conduits running full – Part 5: Cone meters*, Avenue Marnix 17, B-1000 Brussels

Kovacevic, A., Stosic, N. and Smith, I. (2006). Advanced Methods and Tools for Screw Compressor Design. In: *The 6th International Conference TMCE*.

Kovacevic, A., Stosic, N. and Smith, I. (2007). *Screw Compressors - Three Dimensional Computational Fluid Dynamics and Solid Fluid Interaction*. Berlin, Heidelberg: Springer-Verlag Berlin Heidelberg.

Lipták, B. and Lomas, D. (2003). Section 2.1: Application and Selection. In: B. Lipták, ed., *Instrument Engineers' Handbook: Process Measurement and Analysis*, 4th ed. Boca Raton, FL: CRC Press

McAllister, E. (2014). Measurement. *Pipeline Rules of Thumb Handbook*, [online] pp.541-624. Available at: http://www.sciencedirect.com/science/article/pii/B9780123876935000152 [Accessed 27 Jan. 2020].

McCrometer (2008). *Flow Calculations For The V-Cone And Wafer-Cone Flowmeters*. California: McCrometer Inc.

McCrometer (2017). *Exact Steam V-Cone - Installation, Operation And Maintenance Manual.*. Advanced differential Pressure Flowmeter Technology. Lit. # 30122-58, Rev.1.0.

Nakayama, Y. (2018). Measurement of Flow Velocity and Flow Rate. *Introduction to Fluid Mechanics*, pp.215-232.

PCE Instruments (n.d.). *Technical Specification Thermo-Hygrometer PCE-555.*

Saidur, R., Mekhilef, S., Ali, M., Safari, A. and Mohammed, H. (2012). Applications of variable speed drive (VSD) in electrical motors energy savings. *Renewable and Sustainable Energy Reviews*, 16(1), pp.543-550.

Scelzo, M., Milford, S., Mollo, N. and Matson, J. (2005). *Fundamentals Of Ultrasonic Flow Meters*.

Siemens (2020). *Flow Measurement - SITRANS F S Clamp-On*. [online]

Siev, R., Dinapoli, L., Lipták, B. and Yoder, J. (2003). Section 2.26: Ultrasonic flowmeters. In: B. Lipták, ed., *Instrument Engineers' Handbook: Process Measurement and Analysis*, 4th ed. Boca Raton, FL: CRC Press

Stappert, K. (2007). *Application And Verification Of Coriolis Meters For Gas Measurements*. [online] Oklahoma. Available at: <https://asgmt.com/wp-content/uploads/pdf-docs/2007/1/030.pdf> [Accessed 16 April 2020].

Stosic, N., Smith, I., Kovacevic, A. and Mujic, E. (2011). Geometry of screw compressor rotors and their tools. *Journal of Zhejiang University-SCIENCE A,* 12(4), pp.310-326.

Sullair (2012). *Two-Stage Rorary Screw Air Compressors*. Constant Speed and Variable Speed Drives (VSD).

Svenningson, K., Sjölin, U., SRM and Öhman, H. (2010). *The Screw Compressor Development At SRM*.

Texas Instruments (n.d.). *2- 3- 4- Wire RTD (Pt100 to Pt1000) Temperature Measurement*.

The American Society of Mechanical Engineers (ASME) (1998). *ASME PTC 10-1997 (Performance Test Code on Compressors and Exhausters)*. Three Park Avenue, New York, NY 10016-5990. Available at: www.asme.org

The American Society of Mechanical Engineers (ASME) (2006). *ASME PTC 19.1-2005 (Test Uncertainty)*. Three Park Avenue, New York, NY 10016-5990. Available at: www.asme.org

The American Society of Mechanical Engineers (ASME) (2019). *ASME PTC 13-2018 (Wire-to-Air Performance Test Code for Blower Systems)*. Three Park Avenue, New York, NY 10016-5990. Available at: www.asme.org

Transus Instruments (n.d.). *Technical datasheet UIM-4F Metric*.

Tricor Coriolis Technology (n.d.). *Technical datasheet-Classic Series – Tricor Coriolis Mass Flow Meters*.

Tsemekidi-Tzeiranaki, S., Bertoldi, P., Lablanca, N., Castellazzi, L., Ribeiro Serrenho, T., Economidou, M. and Zangheri, P. (2018). *Energy Consumption And Energy Efficiency Trends In The EU-28 For The Period 2000-2016*. Publications Office of the European Union. DOI: 10.2760/574824.

Turunen-Saaresti, T. (2004). *Computational and Experimental Analysis of Flow Field in the Diffusers of Centrifugal Compressors*. PhD thesis, Lappeenranta University of Technology, Department of Energy Technology.

UN General Assembly (2015). *Transforming our world: the 2030 Agenda for sustainable development*. Available at https://www.refworld.org/docid/57b6e3e44.html

U.S. Department of Energy (2014). *Assessment Of The Market For Compressed Air Efficiency Services*. Burlington, Massachusetts: Xenergy, Inc.

Vaisala (2018). *BAROCAP Digital Barometer – PTB330*

Wang, T. and Baker, R. (2014). Coriolis flowmeters: a review of developments over the past 20 years, and an assessment of the state of the art and likely future directions. *Flow Measurement and Instrumentation*, 40, pp.99-123.

Wennemar, J. (2009). Dry screw compressor performance and application range. In: *Thirty-eighth turbomachinery symposium proceedings*. Turbomachinery Laboratory, Texas A&M University, pp.149-156. Available at: https://oaktrust.library.tamu.edu/bitstream/handle/1969.1/163089/ch14_Wennemar.pdf?sequence=1&isAllowed=y

APPENDIX: MEASUREMENT UNCERTAINTY CALCULATION EXAMPLE

The steps followed in deriving the measurement uncertainty in this thesis followed the four steps highlighted in Figure 19 from Chapter 5.1.4. In this appendix, the four steps will be explained in detail with an example calculation.

1: Specify the measurand

2: Identify the uncertainty sources

3: Quantify uncertainty sources and find the partial derivatives

4: Combine the uncertainties

1: SPECIFY THE MEASURAND

The measurand is what is being measured and the utmost measurand of interest in this thesis is the isentropic efficiency of the compressor. A measurand can depend on different input measurands, input quantities, and constants. The isentropic efficiency depends on different measurands and input quantities. The example in this appendix is the isentropic efficiency for a compressor unit where internal compressor measurements are not possible. Here, a mathematical equation (data reduction equation) that equates the isentropic efficiency (η_{is}), as a function of the input parameters is devised as shown in Equation (A.1)

$$\eta_{\mathrm{is}} = \frac{Ideal\ input\ power}{Actual\ input\ power} = \frac{\dot{W}_{\mathrm{is}}}{\dot{W}_{\mathrm{act}}} = \frac{\frac{\kappa}{\kappa-1} q_{\mathrm{m},1} R T_1 (\pi^{\frac{\kappa-1}{\kappa}} - 1)}{\dot{W}_{\mathrm{act}}} . \quad \text{(A.1)}$$

In Equation (A.1), η_{is} is the isentropic efficiency (measurand); the input parameters include isentropic exponent (κ), mass flow at the inlet of the compressor unit ($q_{\mathrm{m},1}$), specific gas constant of the mixture (R), inlet temperature (T_1), pressure ratio (π), and actual input power ($\dot{W}_{\mathrm{act}}$).

2: IDENTIFY THE UNCERTAINTY SOURCES

Here, the sources of uncertainty are identified and listed before they are quantified in step 3. The sources of uncertainty for the isentropic efficiency are thus listed below;

- Isentropic exponent
- Mass flow at the inlet of the compressor unit

- Specific gas constant of the mixture
- Inlet temperature
- Pressure ratio
- Actual input power

3: QUANTIFY UNCERTAINTY AND FIND THE PARTIAL DERIVATIVES

This is done by evaluating the individual uncertainty sources identified in Step 2 for quantification. The sources of uncertainty are directly measured quantities and other measurands.

Direct measurements are;

- The inlet temperature (T_1)
- Actual input power ($\dot{W}_{\mathrm{act}}$)

Other measurands include;

- The mass flow at the inlet of the compressor ($q_{\mathrm{m},1}$), which depends on the measured mass flow at the outlet of the compressor unit, humidity ratio at the inlet and humidity ratio at the outlet of the compressor unit. The humidity ratio at the inlet of the compressor unit subsequently depends on the measured ambient pressure, measured ambient temperature, and measured relative humidity. The humidity ratio at the outlet of the compressor unit depends on the measured pressure and temperature at the outlet of the compressor unit
- The specific gas constant of the mixture (R) depends on the humidity ratio at the inlet of the compressor unit.
- Pressure ratio (π) depends on the pressure at the inlet of the compressor unit and measured pressure at the outlet of the compressor unit.
- Isentropic exponent (κ) depends on the specific gas constant of the mixture and the molar specific heat of the mixture.

Then the partial derivatives are determined in order to estimate how much each input quantity affects the isentropic efficiency. From Equation (A.1), the ideal input power ($\dot{W}_{\mathrm{is}}$) is;

$$\dot{W}_{\mathrm{is}} = \frac{\kappa}{\kappa-1}\, q_{\mathrm{m},1} R T_1 \left(\pi^{\frac{\kappa-1}{\kappa}} - 1\right). \qquad \text{(A.2)}$$

The partial derivatives are then determined as follows;

For isentropic exponent (κ)

$$\frac{\partial \dot{W}_{\mathrm{is}}}{\partial \kappa} = q_{\mathrm{m},1} R T_1 \left[\frac{\partial}{\partial \kappa}\left(\frac{\kappa}{\kappa-1}\right)\left(\pi^{\frac{\kappa-1}{\kappa}}-1\right)+\frac{\partial}{\partial \kappa}\left(\pi^{\frac{\kappa-1}{\kappa}}-1\right)\left(\frac{\kappa}{\kappa-1}\right)\right],$$

while $\frac{\partial}{\partial \kappa}\left(\frac{\kappa}{\kappa-1}\right) = -\frac{1}{(\kappa-1)^2}$,

and $\frac{\partial}{\partial \kappa}\left(\pi^{\frac{\kappa-1}{\kappa}}-1\right) = \frac{e^{\frac{\ln(\pi)(\kappa-1)}{\kappa}\ln(\pi)}}{\kappa^2}$,

$$\frac{\partial \dot{W}_{\mathrm{is}}}{\partial \kappa} = q_{\mathrm{m},1} R T_1 \left[\left(-\frac{1}{(\kappa-1)^2}\right)\left(\pi^{\frac{\kappa-1}{\kappa}}-1\right)+\left(\frac{e^{\frac{\ln(\pi)(\kappa-1)}{\kappa}\ln(\pi)}}{\kappa^2}\right)\left(\frac{\kappa}{\kappa-1}\right)\right],$$

$$\frac{\partial \dot{W}_{\mathrm{is}}}{\partial \kappa} = q_{\mathrm{m},1} R T_1 \left[\left(-\frac{\pi^{\frac{\kappa-1}{\kappa}}-1}{(\kappa-1)^2}\right)+\left(\frac{\pi^{\frac{\kappa-1}{\kappa}}\ln(\pi)}{\kappa(\kappa-1)}\right)\right]. \qquad \text{(A.3)}$$

To get the partial derivate in relative uncertainty terms,

$$\left(\frac{1}{\dot{W}_{\mathrm{is}}}\cdot\frac{\partial \dot{W}_{\mathrm{is}}}{\partial \kappa}\right)u(\kappa) \qquad \text{(A.4)}$$

Substitute in the expressions for $\dot{W}_{\mathrm{is}}$ in Equation (A.2) and $\frac{\partial \dot{W}_{\mathrm{is}}}{\partial \kappa}$ in Equation (A.3) into Equation (A.4)

$$\left[\frac{\kappa-1}{\kappa q_{\mathrm{m},1} R T_1\left(\pi^{\frac{\kappa-1}{\kappa}}-1\right)}\right]\cdot\left[q_{\mathrm{m},1} R T_1\left(\left(-\frac{\pi^{\frac{\kappa-1}{\kappa}}-1}{(\kappa-1)^2}\right)+\left(\frac{\pi^{\frac{\kappa-1}{\kappa}}\ln(\pi)}{\kappa(\kappa-1)}\right)\right)\right]u(\kappa),$$

$$\frac{1}{\kappa}\cdot\left(-\frac{1}{\kappa-1}+\frac{\pi^{\frac{\kappa-1}{\kappa}}\ln(\pi)}{\kappa}\right)u(\kappa),$$

$$\left(-\frac{1}{\kappa-1}+\frac{\pi^{\frac{\kappa-1}{\kappa}}\ln(\pi)}{\kappa}\right)\frac{u(\kappa)}{\kappa}. \qquad \text{(A.5)}$$

For the mass flow at the inlet of the compressor unit

$$\frac{\partial \dot{W}_{\mathrm{is}}}{\partial q_{\mathrm{m},1}} = \frac{\kappa}{\kappa-1} R T_1\left(\pi^{\frac{\kappa-1}{\kappa}}-1\right). \qquad \text{(A.6)}$$

$$\left(\frac{1}{\dot{W}_{\mathrm{is}}}\cdot\frac{\partial\dot{W}_{\mathrm{is}}}{\partial q_{\mathrm{m},1}}\right)u(q_{\mathrm{m},1}),$$

$$\left[\frac{\kappa-1}{\kappa q_{\mathrm{m},1}RT_1\left(\pi^{\frac{\kappa-1}{\kappa}}-1\right)}\right]\cdot\left[\frac{\kappa}{\kappa-1}\,RT_1\left(\pi^{\frac{\kappa-1}{\kappa}}-1\right)\right]u(q_{\mathrm{m},1}),$$

$$\frac{1}{q_{\mathrm{m},1}}\,u\left(q_{\mathrm{m},1}\right)=1\cdot\frac{u(q_{\mathrm{m},1})}{q_{\mathrm{m},1}}. \tag{A.7}$$

For the specific gas constant of the mixture,

$$\frac{\partial\dot{W}_{\mathrm{is}}}{\partial R}=\frac{\kappa}{\kappa-1}\,q_{\mathrm{m},1}T_1\left(\pi^{\frac{\kappa-1}{\kappa}}-1\right). \tag{A.8}$$

$$\left(\frac{1}{\dot{W}_{\mathrm{is}}}\cdot\frac{\partial\dot{W}_{\mathrm{is}}}{\partial R}\right)u(R),$$

$$\left[\frac{\kappa-1}{\kappa q_{\mathrm{m},1}RT_1\left(\pi^{\frac{\kappa-1}{\kappa}}-1\right)}\right]\cdot\left[\frac{\kappa}{\kappa-1}\,q_{\mathrm{m},1}T_1\left(\pi^{\frac{\kappa-1}{\kappa}}-1\right)\right]u(R),$$

$$\frac{1}{R}\,u(R)=1\cdot\frac{u(R)}{R}. \tag{A.9}$$

For the compressor inlet temperature,

$$\frac{\partial\dot{W}_{\mathrm{is}}}{\partial T_1}=\frac{\kappa}{\kappa-1}\,q_{\mathrm{m},1}R\left(\pi^{\frac{\kappa-1}{\kappa}}-1\right). \tag{A.10}$$

$$\left(\frac{1}{\dot{W}_{\mathrm{is}}}\cdot\frac{\partial\dot{W}_{\mathrm{is}}}{\partial T_1}\right)u(T_1),$$

$$\left[\frac{\kappa-1}{\kappa q_{\mathrm{m},1}RT_1\left(\pi^{\frac{\kappa-1}{\kappa}}-1\right)}\right]\cdot\left[\frac{\kappa}{\kappa-1}\,q_{\mathrm{m},1}R\left(\pi^{\frac{\kappa-1}{\kappa}}-1\right)\right]u(T_1),$$

$$\frac{1}{T_1}\,u(T_1)=1\cdot\frac{u(T_1)}{T_1}. \tag{A.11}$$

For the pressure ratio,

$$\frac{\partial \dot{W}_{\mathrm{is}}}{\partial \pi} = \frac{\kappa}{\kappa - 1} q_{\mathrm{m},1} R T_1 \frac{\partial}{\partial \pi}\left(\pi^{\frac{\kappa-1}{\kappa}} - 1\right),$$

while $\frac{\partial}{\partial \pi}\left(\pi^{\frac{\kappa-1}{\kappa}}\right) = \frac{\pi^{\frac{-1}{\kappa}}(\kappa-1)}{\kappa}$,

and $\frac{\partial}{\partial \pi}(1) = 0$,

$$\frac{\partial \dot{W}_{\mathrm{is}}}{\partial \pi} = \left(\frac{\kappa}{\kappa - 1}\right) q_{\mathrm{m},1} R T_1 \left(\frac{\pi^{\frac{-1}{\kappa}}(\kappa-1)}{\kappa} - 0\right),$$

$$\frac{\partial \dot{W}_{\mathrm{is}}}{\partial \pi} = q_{\mathrm{m},1} R T_1 \left(\pi^{\frac{-1}{\kappa}}\right). \tag{A.12}$$

To get the partial derivate in relative uncertainty terms,

$$\left(\frac{1}{\dot{W}_{\mathrm{is}}} \cdot \frac{\partial \dot{W}_{\mathrm{is}}}{\partial \pi}\right) u(\pi)$$

$$\left[\frac{\kappa-1}{\kappa q_{\mathrm{m},1} R T_1\left(\pi^{\frac{\kappa-1}{\kappa}}-1\right)}\right] \cdot \left[q_{\mathrm{m},1} R T_1 \left(\pi^{\frac{-1}{\kappa}}\right)\right] u(\pi),$$

$$\frac{(\kappa-1)\left(\pi^{\frac{-1}{\kappa}}\right)}{\kappa\left(\pi^{\frac{\kappa-1}{\kappa}}-1\right)} u(\pi) = \frac{1}{\pi}\left[\frac{(\kappa-1)\left(\pi^{\frac{-1}{\kappa}}\right)}{\frac{\kappa}{\pi}\frac{\left(\pi^{\frac{\kappa-1}{\kappa}}-1\right)}{\pi}}\right] u(\pi),$$

$$\left[\frac{(\kappa-1)\left(\pi^{\frac{-1}{\kappa}}\right)}{\frac{\kappa}{\pi}\frac{\left(\pi^{\frac{\kappa-1}{\kappa}}-1\right)}{\pi}}\right]\frac{u(\pi)}{\pi}. \tag{A.13}$$

The partial derivatives have now been determined for the ideal input power. The partial derivative for the isentropic efficiency is used to evaluate how the ideal input power and actual input power affects the efficiency.

For the isentropic efficiency,

$$\eta_{\text{is}} = \frac{Ideal\ input\ power}{Actual\ input\ power} = \frac{\dot{W}_{\text{is}}}{\dot{W}_{\text{act}}}. \tag{A.14}$$

For the ideal input power,

$$\frac{\partial \eta_{\text{is}}}{\partial \dot{W}_{\text{is}}} = \frac{1}{\dot{W}_{\text{act}}}. \tag{A.15}$$

$$\frac{1}{\eta_{\text{is}}} \cdot \frac{\partial \eta_{\text{is}}}{\partial \dot{W}_{\text{is}}} u(\dot{W}_{\text{is}}) = \frac{\dot{W}_{\text{act}}}{\dot{W}_{\text{is}}} \cdot \frac{1}{\dot{W}_{\text{act}}} u(\dot{W}_{\text{is}}) = \frac{1}{\dot{W}_{\text{is}}} u(\dot{W}_{\text{is}}),$$

$$1 \cdot \frac{u(\dot{W}_{\text{is}})}{\dot{W}_{\text{is}}}. \tag{A.16}$$

For the actual input power,

$$\frac{\partial \eta_{\text{is}}}{\partial \dot{W}_{\text{act}}} = -\frac{\dot{W}_{\text{is}}}{(\dot{W}_{\text{act}})^2}. \tag{A.17}$$

$$\frac{1}{\eta_{\text{is}}} \cdot \frac{\partial \eta_{\text{is}}}{\partial \dot{W}_{\text{act}}} u(\dot{W}_{\text{act}}) = \frac{\dot{W}_{\text{act}}}{\dot{W}_{\text{is}}} \cdot \left(-\frac{\dot{W}_{\text{is}}}{(\dot{W}_{\text{act}})^2} \right) u(\dot{W}_{\text{act}}) = -\frac{1}{\dot{W}_{\text{act}}} u(\dot{W}_{\text{act}}),$$

$$-1 \cdot \frac{u(\dot{W}_{\text{act}})}{\dot{W}_{\text{act}}}. \tag{A.18}$$

4: COMBINE THE UNCERTAINTIES

This is the last step where the uncertainties are combined using the propagation of errors. The expanded uncertainty at 95% confidence interval is also determined by using a coverage factor of 2. In this example, some estimated and precalculated values shown in Table A.1 are inserted into the Equations to determine the uncertainty of the isentropic efficiency.

Table A.1. Estimated values used in the equations

Quantity	**Value**
Relative uncertainty in isentropic exponent, $\frac{u(\kappa)}{\kappa}$	0.68%
Relative uncertainty in inlet mass flow, $\frac{u(q_{\mathrm{m},1})}{q_{\mathrm{m},1}}$	0.5%
Relative uncertainty in specific gas constant of the mixture, $\frac{u(R)}{R}$	1.21%
Relative uncertainty in inlet temperature, $\frac{u(T_1)}{T_1}$	0.5%
Relative uncertainty in pressure ratio, $\frac{u(\pi)}{\pi}$	0.13%
Relative uncertainty in actual input power, $\frac{u(\dot{W}_{\mathrm{act}})}{\dot{W}_{\mathrm{act}}}$	0.2%
Isentropic exponent, κ	1.4
Pressure ratio, π	2.78

Combining the uncertainties for the ideal input power

$$\frac{u(\dot{W}_{\mathrm{is}})}{\dot{W}_{\mathrm{is}}} = \sqrt{\begin{array}{c}\left[\left(\frac{\partial \dot{W}_{\mathrm{is}}}{\partial \kappa}\right)^2 \cdot \left(\frac{u(\kappa)}{\kappa}\right)^2\right] + \left[\left(\frac{\partial \dot{W}_{\mathrm{is}}}{\partial q_{\mathrm{m},1}}\right)^2 \cdot \left(\frac{u(q_{\mathrm{m},1})}{q_{\mathrm{m},1}}\right)^2\right] + \left[\left(\frac{\partial \dot{W}_{\mathrm{is}}}{\partial R}\right)^2 \cdot \left(\frac{u(R)}{R}\right)^2\right] \\ + \left[\left(\frac{\partial \dot{W}_{\mathrm{is}}}{\partial T_1}\right)^2 \cdot \left(\frac{u(T_1)}{T_1}\right)^2\right] + \left[\left(\frac{\partial \dot{W}_{\mathrm{is}}}{\partial \pi}\right)^2 \cdot \left(\frac{u(\pi)}{\pi}\right)^2\right]\end{array}} \quad \text{(A.19)}$$

Substituting the partial derivatives into Equation (A.19)

$$\frac{u(\dot{W}_{\mathrm{is}})}{\dot{W}_{\mathrm{is}}} = \sqrt{\begin{matrix}\left[\left(-\frac{1}{\kappa-1}+\frac{\pi^{\frac{\kappa-1}{\kappa}}\ln(\pi)}{\kappa}\right)^2\cdot\left(\frac{u(\kappa)}{\kappa}\right)^2\right]+\left[1^2\cdot\left(\frac{u(q_{\mathrm{m},1})}{q_{\mathrm{m},1}}\right)^2\right]+\left[1^2\cdot\left(\frac{u(R)}{R}\right)^2\right] \\ +\left[1^2\cdot\left(\frac{u(T_1)}{T_1}\right)^2\right]+\left[\left(\frac{(\kappa-1)\left(\pi^{\frac{-1}{\kappa}}\right)}{\frac{\kappa}{\pi}\left(\frac{\pi^{\frac{\kappa-1}{\kappa}}-1}{\pi}\right)}\right)^2\cdot\left(\frac{u(\pi)}{\pi}\right)^2\right]\end{matrix}}$$

Substitute in the values from Table A.1.

$$\frac{u(\dot{W}_{\mathrm{is}})}{\dot{W}_{\mathrm{is}}} = \sqrt{\begin{matrix}\left[\left(-\frac{1}{1.4-1}+\frac{2.78^{\frac{1.4-1}{1.4}}\ln(2.78)}{1.4}\right)^2\cdot(0.68\%)^2\right]+[1^2\cdot(0.5\%)^2]+[1^2\cdot(1.21\%)^2] \\ +[1^2\cdot(0.5\%)^2]+\left[\left(\frac{(1.4-1)\left(2.78^{\frac{-1}{1.4}}\right)}{\frac{1.4}{2.78}\left(\frac{2.78^{\frac{1.4-1}{1.4}}-1}{2.78}\right)}\right)^2\cdot(0.13\%)^2\right]\end{matrix}}$$

$$\frac{u(\dot{W}_{\mathrm{is}})}{\dot{W}_{\mathrm{is}}} = \sqrt{\begin{matrix}[-1.522^2\cdot(0.68\%)^2]+[1^2\cdot(0.5\%)^2]+[1^2\cdot(1.21\%)^2] \\ +[1^2\cdot 0.5\%)^2]+[3.135^2\cdot(0.13\%)^2]\end{matrix}}$$

$$\frac{u(\dot{W}_{\mathrm{is}})}{\dot{W}_{\mathrm{is}}} = \sqrt{(2.357 * 10\text{^} - 4)} = \pm 2.14\%$$

Then combining the ideal input power and actual input power uncertainties using Equation (A.20) for the isentropic efficiency. Then substitute in the $\frac{u(\dot{W}_{is})}{\dot{W}_{is}}$ result and $\frac{u(\dot{W}_{act})}{\dot{W}_{act}}$ from Table A.1.

$$\frac{u(\eta_{is})}{\eta_{is}} = \sqrt{\left[\left(\frac{\partial \eta_{is}}{\partial \dot{W}_{is}}\right)^2 \cdot \left(\frac{u(\dot{W}_{is})}{\dot{W}_{is}}\right)^2\right] + \left[\left(\frac{\partial \eta_{is}}{\partial \dot{W}_{act}}\right)^2 \cdot \left(\frac{u(\dot{W}_{act})}{\dot{W}_{act}}\right)^2\right]} \quad \text{(A.20)}$$

$$\frac{u(\eta_{is})}{\eta_{is}} = \sqrt{\left[1^2 \cdot \left(\frac{u(\dot{W}_{is})}{\dot{W}_{is}}\right)^2\right] + \left[-1^2 \cdot \left(\frac{u(\dot{W}_{act})}{\dot{W}_{act}}\right)^2\right]}$$

$$\frac{u(\eta_{is})}{\eta_{is}} = \sqrt{[1^2 \cdot (2.14\%)^2] + [-1^2 \cdot (0.2\%)^2]} = \sqrt{(4.54 * 10^{-4})} = \pm 2.13\%$$

Then the expanded uncertainty at 95% confidence interval can be determined using Equation (A.21) below.

$$U_{\eta_{is},95} = 2 \cdot \frac{u(\eta_{is})}{\eta_{is}} \quad \text{(A.21)}$$

$$U_{\eta_{is},95} = 2 \cdot 2.13\% = \pm 4.26\%$$

The measurement uncertainty for determining the isentropic efficiency is thus $\pm 4.26\%$.